Joint Activity Scenarios and Modelling

Swiss Energy Scope – ETH

Swiss Energy Scope with hourly resolution

Adriana Marcucci
Gianfranco Guidati
Domenico Giardini

ETH Zurich

January 15, 2021

Supported by:

Schweizerische Eidgenossenschaft
Confédération suisse
Confederazione Svizzera
Confederaziun svizra

Swiss Confederation

Innosuisse – Swiss Innovation Agency

Contents

Chapter 1

Model description

The Swiss Energyscope - ETH (SES-ETH) model was developed at ETH Zurich based on the original model by Stefano Moret from EPFL (Moret, 2017). SES is a linear optimization model of the energy system. It determines the investment and operation strategies that minimize the total annual cost, given the end-use energy demand; the efficiency and costs of the conversion technologies; and the availability and costs of the energy resources.

SES represents the main energy demands: electricity, heating and mobility. SES is a snapshot model, that is, it models the energy system in a target year and it does not make any statements on the trajectory to reach this future state. To model this target year, the original SES (Moret, 2017) included multiple periods that could capture seasonality and energy storage options. We have further developed the model to include an hourly resolution that allows us to represent the intra-day variations of the energy demand and resource availability.

SES is a simple representation of the energy system, it largely neglects all aspects of spatial resolution, and it reduces the temporal resolution by choosing typical days and clustering hours within a day. These simplifications do not hinder the ability of the SES-ETH model to make inferences; on the contrary, by reducing the dimensionality, we are able to analyze large sets of scenarios considering uncertainty of modelling inputs. What we lose in granularity we gain in model tractability and the ability to identify technologies that are very likely part of the future mix and to derive policy recommendations for today.

Figure 1.1 illustrates the SES-ETH structure. Imported and domestic resources (Chapter 2) can be converted with energy conversion technologies (Chapter 4) to satisfy end-use demand in energy services: electricity, low and high temperature heat (LTH and HTH), and mobility (passenger and freight) (Chapter 3). The model represents the energy conversion processes and determines the optimal technology mix for a certain emissions target by minimizing the total system costs. In the following sections we describe the different components of SES-ETH: First, the objective function; second, we describe how we model the conversion processes through balancing inputs and outputs in every layer (Section 1.2; third, we describe the representation of CO_2 streams; fourth, we present the modelling of seasonal and intra-day variations through typical days and intra-day clusters (Section 1.4); and finally we show some additional constraints that we use in the model.

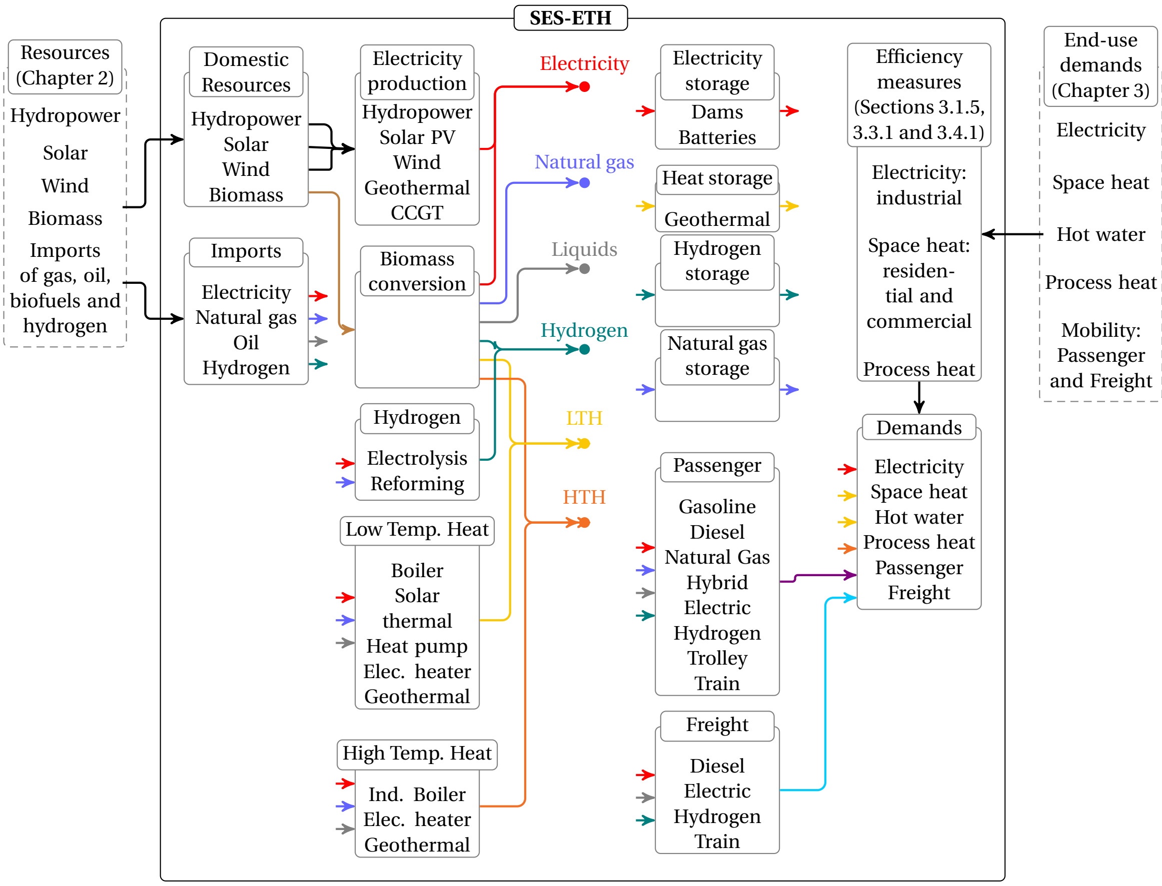

Figure 1.1: SES-ETH structure. LTH: Low temperature heat, HTH: High temperature heat.

1.1 Objective function

The objective function of the SES-ETH model is the miminization of the discounted total system costs. These costs include investment and operating costs for technologies, C_T, and extraction (or import) costs for resources, C_R, thus,

$$\min \frac{1}{(1+\rho)^n}\left(C_T + C_R\right), \tag{1.1}$$

where ρ is the discount rate and n is the number of years between today and the target year.

The first term in Equation 1.1 corresponds to the costs of investing in and using certain technologies for both energy production and storage, thus,

$$C_T = \sum_{i \in \text{Technologies}} (inv_i + om_i)\, F_i \quad + \sum_{\substack{i \in \text{Hourly} \\ \text{storage tech.}}} (inv_i + om_i) \sum_{l \in \text{Layers}} S_{i,l} \quad + multfac \cdot \sum_{\substack{i \in \text{Seasonal} \\ \text{storage tech.}}} (inv_i + om_i) \sum_{l \in \text{Layers}} S_{i,l},$$

where inv_i and om_i are the specific investment and operating cost (in CHF/MW) of the ith-technology, respectively; F_i is the installed capacity of the ith-technology; $S_{i,l}$ is the installed storage capacity of layer l using the ith-technology. In SES-ETH, we assume that the year consists only of $n_{typical}$ typical days. Hence, we need to upscale the level of installed capacity of seasonal storage by $multfac = 360/n_{typical}$ (Section 1.4.2).

The second term in Equation 1.1 represents the costs of using certain resources, thus,

$$C_R = multfac \cdot \sum_{i \in \text{Resources}} rsc_i \sum_{t \in \text{periods}} F_{i,t},$$

where rsc_i is the import or extraction cost of the ith-resource (in CHF/kWh); $F_{i,t}$ is the use of the i-th resource in period t; and *multfac* is the correction factor for the use of typical days (Section 1.4.2).

1.2 Layers

Layers are resources and end-use demands. Inputs and outputs from and to technologies (conversion and resource extraction technologies) need to be balanced in each period. Resource technologies are extraction of domestic resources or imports; while conversion technologies represent processes that transform energy carriers into other energy carriers or end-use demands.

Table 1.1: Example of matrix f that relates technologies to layers

	Layers				
	Gas	Wood	Electricity	HTH	LTH
Resource technologies					
Gas import	1	0	0	0	0
Wood harvest	0	1	0	0	0
Conversion technologies					
Gas turbine	-1.59	0	1	0	0
Wood power plant	0	-4.17	1	0	0
Wood Gasification	1	-1.74	0	0	0
Gas industrial burner	-1.08	0	0	1	0
Wood industrial burner	0	-1.33	0	1	0
Gas boiler	-1.11	0	0	0	1
Wood boiler	0	-1.43	0	0	1

We balance the layers using the matrix f that relates technologies to layers. Every row in f represents a technology that produces and uses different elements in the layers. For example, imagine the simple energy system with the matrix f in Table 1.1. This system has five layers: two resources (gas and wood) and three end-use demands (electricity and high and low temperature heat). The rows correspond to the following technologies:

- Resource technologies: One unit of imported gas produces one unit of gas in the system. In the same way, one unit of harvested wood corresponds to one unit of wood in the system. There are no efficiency losses.
- Conversion technologies:

1. A gas turbine, for instance, requires 1.59 units of gas to produce 1 unit of electricity, which means an efficiency of 63%.
2. A wood power plant, requires 4.17 units of wood to produce 1 unit of electricity, which means an efficiency of 24%.
3. At the same time, wood can be used by a gasifier to produce gas with an efficiency of $1/1.74 = 57\%$.
4. Gas and wood industrial burners produce high temperature heat (HTH) with efficiencies: $1/1.08 = 92.5\%$ and $1/1.23 = 81\%$, respectively.
5. Finally, wood and gas boilers produce low temperature heat (LTH) with efficiencies: $1/1.11 = 90\%$ and $1/1.43 = 70\%$, respectively.

Besides resources and conversion technologies, we include seasonal and hourly storage technologies, like hot water storage in a house. Storage technologies allow storage across seasons or days. The storage is modeled as a "tank" whose level (S_t) in period t is equal to the level at the end of the previous period plus the input to the storage (*Sin*) minus the output (*Sout*) in t, thus,

$$S_{i,l,t} = S_{i,l,t-1} + h\left(\eta^{in}_{i,l} Sin_{i,l,t} - \frac{Sout_{i,l,t}}{\eta^{out}_{i,l}}\right) \qquad \forall i \in \text{Storage technologies}, l \in \text{Layers}, \tag{1.2}$$

where $\eta^{in}_{i,l}$ and $\eta^{out}_{i,l}$ are the efficiencies for input and output, respectively; and h is the number of hours in period t (Section 1.4.1). *Sout* is the amount of energy the system receives, hence, the amount of energy withdrawn from the reservoir is larger and corresponds to *Sout* divided by the efficiency $\eta^{out}_{i,l}$.

The model determines the energy production, $F_{i,t}$, of the i-th technology in every period t by balancing resource and conversion technologies, demand and storage of every layer, hence,

$$\sum_{\substack{i \in \text{Resources} \\ +\text{Technologies}}} f_{i,l} F_{i,t} + \sum_{i \in \text{Storage tech.}} \left(Sout_{i,l,t} - Sin_{i,l,t}\right) = \frac{demand_{l,t}}{multfac} \qquad \forall l \in \text{Layers}, \tag{1.3}$$

where $f_{i,l}$ is the element in the matrix f that relates the i-th technology to the l-th layer; $F_{i,t}$ is the production in period t of the i-th technology; $Sin_{i,l,t}$ and $Sout_{i,l,t}$ are the input from and output to the i-th reservoir; $demand_{l,t}$ is the system demand of the l-th layer in period t (zero in the case of resources); and *multfac* is the correction factor for the use of typical days (Section 1.4.2).

The total production in each period t of the i-th technology ($F_{i,t}$) is limited by the maximum production of the technology, i.e. the installed capacity, multiplied by the time dependent capacity factor (cf), thus,

$$F_{i,t} \leq F_i \cdot cf_{i,t} \qquad \forall i \in \text{Technologies}.$$

The capacity factor allows us to control the output of technologies such as photovoltaics or wind. It is one for those technologies that can be dispatched freely. In the same way, the storage level in each period t of the i-th storage technology is limited by the maximum storage level of the technology, i.e. the installed storage capacity, thus,

$$S_{i,l,t} \leq S_{i,l} \qquad \forall i \in \text{Technologies}, l \in \text{Layers}.$$

1.3 CO_2 streams

Table 1.2: Example of matrix f for CO_2 layers

	Layers			
	Latent	Flue gas	Pure	To atmosphere
Resource technologies				
Gas import	0.2	0	0	0
Wood harvest	0.36	0	0	0
Technologies				
Gas turbine	-1.59×0.2	1.59×0.2	0	0
Wood power plant	-4.17×0.36	4.17×0.36	0	0
Wood Gasification	$-1.74 \times 0.36 + 0.2$	0	$1.74 \times 0.36 - 0.2$	0
Gas industrial burner	-1.08×0.2	0	0	1.08×0.2
Wood industrial burner	-1.33×0.36	0	0	1.33×0.36
Gas boiler	-1.11×0.2	0	0	1.11×0.2
Wood boiler	-1.43×0.36	0	0	1.43×0.36
CO2 separation	0	-1.11	1	0.11

Any physical energy stream such as gas or wood carries a corresponding CO_2 stream that is released when the energy stream undergoes a chemical transformation such as combustion or gasification. We consider four types of CO_2 streams:

- Latent CO_2, i.e. the CO_2 that is inherent to a physical energy carrier;
- CO_2 in a flue gas, i.e. a mixture of air (mostly nitrogen) and CO_2 that results normally from combustion. In the flue gas, CO_2 can, in principle, be captured by separation;
- CO_2 that is directly released to the atmosphere and cannot be captured, for instance from a vehicle or a domestic boiler;
- Pure CO_2 that either results directly from a process such as autothermal gasification or from the separation from a flue gas.

We represent these four types of CO_2 streams as layers that are balanced with the layers balancing equation (Equation 1.3). Table 1.2 presents the matrix f for the CO_2 layers in the simple energy system described in Section 1.2:

1. One unit of gas contains 0.2 kg_{CO2}/kWh, which goes to the latent CO_2 layer, i.e. it is inherent to the resource. One unit of wood, contains 0.36 kg_{CO2}/kWh.
2. A gas turbine extracts 1.59×0.2 kg_{CO2}/kWh to produce one unit of electricity, given the efficiency of $1/1.59$ represented by the f matrix in Table 1.1.

3. A special case is wood gasification to gas. This technology *removes* CO_2 from the latent stream by consuming wood (with an efficiency of 1/1.74) but it also *adds* to the latent stream in the form of gas (+0.2 kg_{CO2}/kWh). The resulting balance ends up in the pure stream (assuming a hypothetical autothermal reforming process).

4. Gas and wood boiler burners and boilers move CO_2 from the latent stream directly to the atmosphere, here no CO_2 capture is foreseen.

5. Finally, all CO_2 in the flue gas stream can be captured by a CO_2 separation technology (last row in Table 1.2). We assume a capture rate of 90% for this technology. Hence, it takes 1.11 units of CO_2 from the flue gas and supplies 1 unit of CO_2 to the pure stream and 0.11 units to the the atmosphere stream.

1.4 Periods: seasonal and intra-day variation

The original version of Swiss Energyscope (Moret, 2017) had a monthly time resolution. This allowed us to model seasonal variations but neglected the intra-day variation. The alternative to go for a full resolution of 8760 hours per year is not possible, especially since we use SES-ETH mainly for Monte Carlo analyses that require thousands of evaluations. Therefore, to represent seasonal and intra-day variation while limiting computation time we used two approaches: (i) an intra-day clustering, and (ii) modelling of typical days.

1.4.1 Intra-day clustering

We use intra-day clustering to reduce the complexity of the model while capturing intra-day variations. We cluster together a number h of hours of the day and treat them as a single time step. We assume that the largest size of the clusters is h=8 hours, which allow us to represent the fact that photovoltaic generation is available in the middle of the day and not during the early morning, the evening and the night. Other clustering schemes are 8 clusters of h=3 hours and 24 clusters of h=1 hour, i.e. no clustering.

With the inta-day clustering the periods in SES-ETH correspond to blocks of h hours in the typical days. Therefore, we need to apply a correction factor to all variables that are defined at the hour scale, i.e. we multiply by h.

1.4.2 Typical days

We use typical days to represent the seasonal variation in the energy system. Our procedure consists in: (1) defining a number of typical days ($n_{typical}$); (2) dividing the year into $n_{typical}$ clusters of days; and (3) determining the day that better represents all days inside the cluster. In contrast to other typical day approaches, we assume that the year consists of the number of typical days ($n_{typical}$) only, e.g. 12, 24 or 36 days. Therefore, the periods in SES-ETH correspond to blocks of hours in typical days. For example, blocks of 8 hours (h) in 12 typical days ($n_{typical}$) imply $n_{periods} = n_{typical} \times \frac{24}{h} = 36$.

Procedure to find the typical days

Full 8760 hour time series are available for the different demands and renewable potentials, e.g. space heating and photovoltaics. We simplify the split into typical days by reducing the year to 8640 hours or 360 days. We define first the number of typical days, $n_{typical}$. We split the 360 days into $n_{typical}$ slices with $d_{slice} = \frac{8640}{24 \cdot n_{typical}}$ days. For instance, if we have $n_{typical} = 24$, each contains $d_{slice} = 15$ days. Within each one of the slices, one of the d_{slice} days is selected as the typical day according to two criteria: (i) minimum distance to the average of the slice, and (ii) minimum error in the total duration curve. The duration curve plots the variable (demand or resource availability) versus the hours of the year, arranging the hours in descending order, so that the peak value of the year appears in the left of the plot. These two criteria allow us to choose the day that better represents the variation during the day, the seasons and the peak values.

We solve the problem is two steps. First, for each slide s, we find the set of "best days" among the d_{slice} days of the slice, $BD_s = \{d_{s,1}, d_{s,2}, \dots d_{s,n_{best}}\}$. These days are those with the minimum distance to the hourly average of the slice, given by,

$$\|x_{d_{s,i}} - \overline{x}_s\| \qquad \forall s \in \{1 \dots n_{typical}\},$$

where $x_{d_{s,i}}$ is demand of the $d_{s,i}$-th day and $\overline{x}_s$ is the average hourly demand of the slice s.

Once we have the set of "best days", we find the combination of days that minimizes the error in the total duration curve.

$$\min_{d_{s,i} \in BD_s} \|dc_{d_{s,i}} - dc\| \forall s \in \{1 \dots n_{typical}\},$$

where $dc_{d_{s,i}}$ is the duration curve replacing all days in slice s with $d_{s,i}$ and dc is the original duration curve of the data.

Corrections due to the use of typical days

In our approach we assume that the year consists of the number of typical days only. This simplification requires some corrections in the model. Any resource that is supplied to the model, e.g. the total amount of available wood is *scaled down* by a factor $multfac = 360/n_{typical}$. All the results that are calculated over a year, such as the yearly electricity production, are *scaled up* by the same factor. Seasonal storage of a given volume needs to be scaled down. As an example, the Swiss storage volume of the hydro reservoirs is 8.8 TWh. In a 24 typical days setting, this is scaled down by a factor of 360/24. Finally, to avoid energy transfers between typical days (leak from one typical day to another), we force the level of the hourly storage in the last hour of each typical day to be the same level as in the first hour of the day.

Validation of typical days

Using this approach we can split the year into any number of typical days. As an example, we calculate 24 typical days for space heating demand (single family houses, old, the original time series in shown in Figure 1.2a). To validate the choice of the typical days, we first compare the typical days to the average profile of the corresponding days in Figure 1.2b and we see that the chosen typical days are close to the average. Third, we compare the duration curve of the original data and the typical days in Figure 1.2c. Finally, we calculate a seasonal curve that corresponds to the average over the 24 hours and 15 days (see 1.2d). Overall, the main features of the intra-day and seasonal variation are preserved when using the 24-typical days.

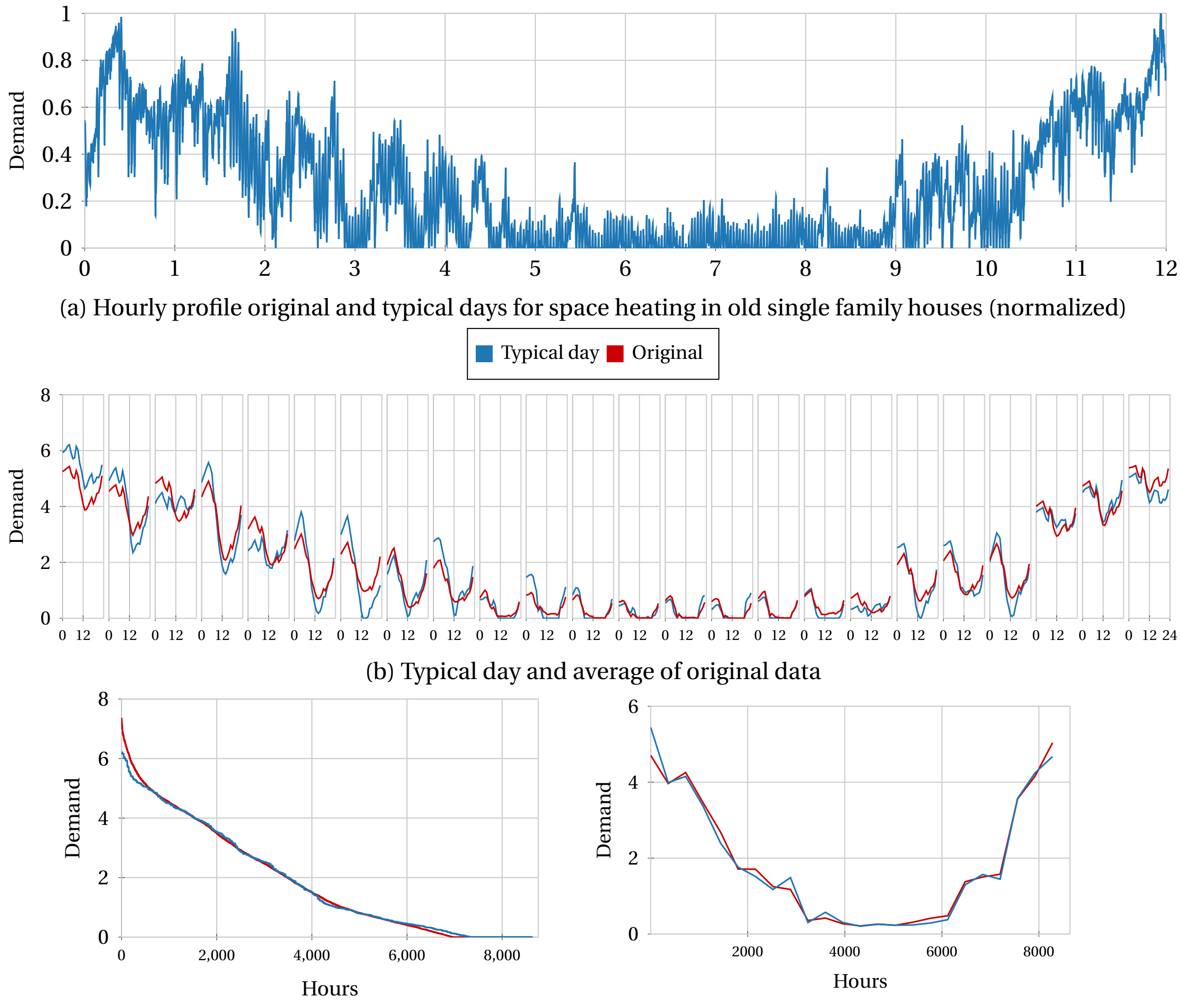

(a) Hourly profile original and typical days for space heating in old single family houses (normalized)

(b) Typical day and average of original data

(c) Duration curve typical day and original data

(d) Seasonal curve typical day and original data

Figure 1.2: Validation plots of typical days for space heating in old single family houses

Appendix A.1 discusses the effect of the choice of the number of typical days and intra-day cluster on the results.

1.5 Yearly Constraints

1.5.1 Resource availability

The yearly use of the i-th resource is limited by its yearly availability ($avail_i$), thus,

$$\sum_t F_{i,t} \cdot h \leq \frac{avail_i}{multfac} \qquad \forall i \in \text{Resources},$$

where $F_{i,t}$ is the use of the i-th resource in period t; h is the number of hours in period t (Section 1.4.1); and *multfac* is the correction factor for the use of typical days (Section 1.4.2). Since $avail_i$ is the yearly availability, we use both h and *multfac* to correct for both the intra-day clustering and the typical days.

1.5.2 Minimum and maximum capacities

Upper and lower limits to the total installed capacity of each technology are set by *fmax* and *fmin*, respectively, thus,

$$\begin{aligned} fmin_i \leq F_i \leq fmax_i & \qquad \forall i \in \text{Technologies} \\ fmin_i \leq multfac \cdot S_{i,l} \leq fmax_i & \qquad \forall i \in \text{Seasonal Storage Technologies} \\ fmin_i \leq S_{i,l} \leq fmax_i & \qquad \forall i \in \text{Hourly Storage Technologies,} \end{aligned}$$

where F_i is the installed capacity of the i-th technology; $S_{i,l}$ is the installed storage capacity of layer l using the ith-technology; and $multfac$ is the correction factor due to the use of typical days (Section 1.4.2).

Chapter 2

Resources

This chapter describes the exogenous assumptions on resources in the SES-ETH. Zooming-in Figure 1.1, we refer to the left part of the structure of the model (Figure 2.1).

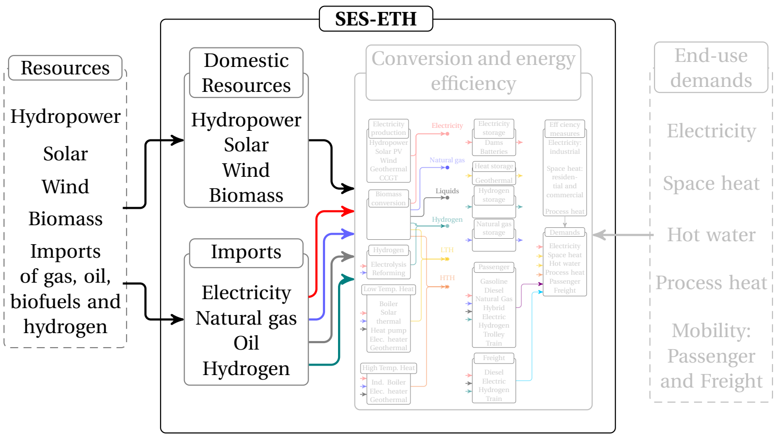

Figure 2.1: SES-ETH structure: Resources

2.1 Biomass and waste potentials

Biomass and waste are important resources to the future Swiss Energy System. ETH and Biosweet estimated the potentials of the different biomass resources and waste for the use in the energy system (Guidati et al., 2020) (see Table 2.1).

Table 2.1: Energy potential of biomass and waste categories in the reference variant in PJ

		Energy Potential (PJ)									
Category	**Feedstock**	**2015**	**2020**	**2025**	**2030**	**2035**	**2040**	**2045**	**2050**	**2055**	**2060**
(A) Wood	Forest wood										
	Scenario (1)	17.1	20.1	23.0	26.0	26.0	26.0	26.0	26.0	26.0	26.0
	Scenario (2)	17.1	22.2	27.2	32.3	32.3	32.3	32.3	32.3	32.3	32.3
	Scenario (3)	17.1	24.5	31.9	39.4	39.4	39.4	39.4	39.4	39.4	39.4

Table 2.1: Energy potential of biomass and waste categories in the reference variant in PJ (continued)

		Energy Potential (PJ)									
Category	**Feedstock**	**2015**	**2020**	**2025**	**2030**	**2035**	**2040**	**2045**	**2050**	**2055**	**2060**
	Wood from landscape	2.3	3.2	4.0	4.8	4.8	4.8	4.8	4.8	4.8	4.8
	Wood residues	7.4	7.5	7.6	7.7	7.7	7.7	7.7	7.7	7.7	7.7
	Waste wood	9.1	11.1	13.2	15.3	15.9	16.3	16.6	17.0	17.3	17.6
(B) Manure	Animal manure (dry)	2.5	10.5	18.4	26.3	26.3	26.3	26.3	26.3	26.3	26.3
(C) Green waste	Collected organic waste	3.3	3.9	4.6	5.4	6.2	7.1	8.1	9.1	10.1	11.2
	Agricultural byproducts	0.1	0.9	1.8	2.6	2.6	2.6	2.6	2.6	2.6	2.6
(D) Sewage sludge	Fresh sewage sludge (dry)	4.9	5.1	5.3	5.5	5.7	5.8	6.0	6.1	6.2	6.3
(E) Mixed fossil/	Imports	4.2	2.8	1.4	0.0	0.0	0.0	0.0	0.0	0.0	0.0
organic waste	Export	5.9	3.3	1.7	0.0	0.0	0.0	0.0	0.0	0.0	0.0
	Other waste fraction	22.8	24.7	27.3	29.8	31.6	33.1	34.5	35.9	37.1	38.5
	Municipal waste	31.4	30.9	31.4	31.9	32.1	32.1	31.9	31.7	31.3	30.9
	including green waste	*2.8*	*2.5*	*2.4*	*2.2*	*2*	*1.7*	*1.5*	*1.2*	*0.9*	*0.6*

Data available at https://data.sccer-jasm.ch/biomass-potentials/

The potentials estimated in Guidati et al. (2020) include three different wood potential scenarios depending on economic restrictions and the management policy. Figure 2.2 depicts the potentials in the reference variant for the three wood scenarios. Total potentials of biomass excluding mixed waste are in the range of 98.3–120.2 PJ in 2060. Waste potentials are projected to be 70 PJ by 2060.

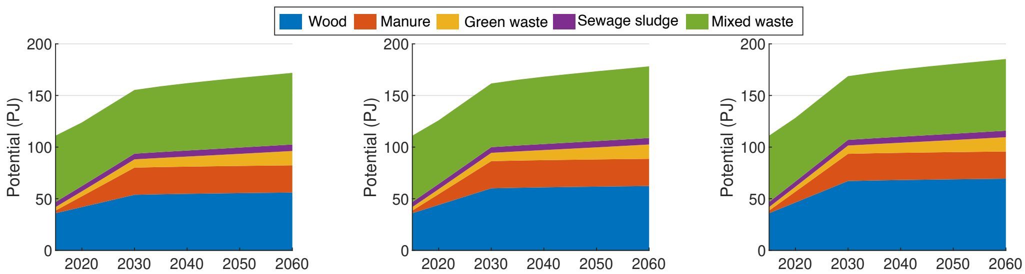

(a) Low wood (b) Medium wood (c) High wood

Figure 2.2: Biomass and waste potentials for the reference variant

2.2 Hydropower

Hydropower is the backbone of the Swiss electricity system, supplying around 60% of today's electricity. Roughly half of it is produced with run-of-river power stations and the other half with storage lakes. While run-of-river (RoR) power plants are not dispatchable, storage plants are highly flexible at time scales ranging from hours to days and even months.

2.2.1 Expected annual production

SCCER-SoE (2020) estimates a long term hydropower production in 2050 of 36 TWh/a. This amount considers already that the production during the last years was higher due to an absolute reduction of glacier volume. The analysis by SCCER-SoE (2020) also studied the effect of different factors on the hydropower potential, including increased residual flows, protection to fish migration, refurbishment of existing plants, and construction of new plants. Table 2.2 shows that these factors lead to a large uncertainty of roughly +/- 10%. As shown in the next section, climate change does impact the monthly distribution of inflows to RoR plants and storage lakes. The analysis shows also that the absolute numbers are not significantly impacted at least during the first middle of the century. Only towards the end of the 21st century there will likely be a reduction in available hydropower, especially for the most impacting RCP 8.5 climate scenario.

Table 2.2: Impact of various factors on annual hydropower production in 2050 (SCCER-SoE, 2020)

	Change in TWh/a		
Impact category	**Pessimistic**	**Medium**	**Optimistic**
Increased residual flows	-3.6	-2.3	-1.9
Measures to protect fish migration	-1.0	-0.4	-0.2
Refurbishment of existing plants	+0.4	+0.8	+2.0
New plants	+1.1	+2.3	+3.1
Total	**-3.1**	**+0.4**	**+3.0**

2.2.2 Monthly distribution and impacts of climate change

Monthly statistics for hydropower production can be found at SFOE (BFE, 2017a, 2019a). The available data includes the production of storage and RoR plants, the consumption of pump storage plants, and the level of storage lakes, all expressed in energy units (TWh). The inflow data is exogenous in the sense that it cannot be influenced by the operator (similar to the solar irradiation for photovoltaics).

We model RoR plants and storage lakes. In the case of RoR plants, the production is proportional to the inflow coming from the rivers and the operator has little control. Therefore, we can use directly the time series of the historical production. In the case of storage plants, the operator has greater influence in production choices. Thus, the production time series is a result of the inflow to the storage lakes and the operation concept of the operator (that is limited by the volume of the storage lakes). Since we want to analyze possible future changes to the operation of the power plants, we need the inflow to the storage lakes as input to the model. This quantity cannot be found usually in the SFOE statistics. We can, however, reconstruct the inflow to the storage lakes $P_{lake,in}$ by making an energy balance for the storage lakes:

$$\frac{\Delta E_{lake}}{\Delta T} = P_{lake,in} - P_{lake} + P_{pump} \cdot \eta_{pump}, \tag{2.1}$$

where $\frac{\Delta E_{lake}}{\Delta T}$ is the change in the level of the storage lakes in one period, P_{lake} is the production of the storage lakes; and P_{pump} and η_{pump} are the production and efficiency of the pumped hydropower plants.

The total inflow P_{in} is the sum of the inflow to RoR power plants $P_{RoR,in}$ and the inflow to the storage lakes $P_{lake,in}$, thus,

$$P_{in} = P_{RoR,in} + P_{lake,in} \tag{2.2}$$

We need to add an important caveat to this analysis. The water that is available to the RoR plants is partly coming from the storage lakes, i.e. in reality the two technologies and the respective production time series are not independent of each other. Whenever a storage power plant produces electricity, the water is discharged downstream and will eventually also pass through a run-of-river plant. However, power generation per cubic meter is much higher for a storage plant due to higher head. Therefore, we model RoR and storage power plants as two separated entities. RoR plants transform the water flow into electricity at the moment the water inflow arrives (or curtailed like PV and wind). Storage plants, on the other hand, accumulate water in the storage lakes. This water can be turned into electricity at any time, considering of course the limitations of the storage lake itself.

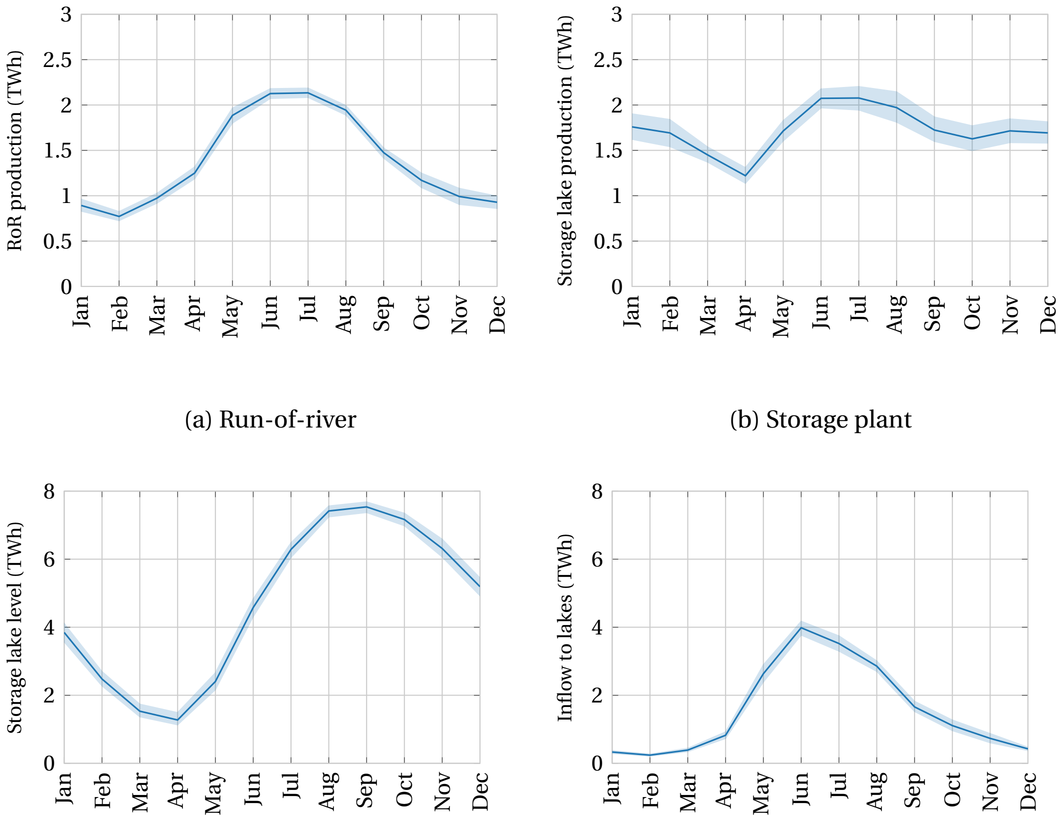

(a) Run-of-river

(b) Storage plant

(c) Storage lake level

(d) Inflow to lakes

Figure 2.3: Monthly generation in Swiss hydropower system 2000-2018 (TWh) (BFE, 2019b)

Typical generation patterns of today are shown in Figure 2.3 (showing the median and 25/75 percentiles for the years 2000 to 2018). Run-of-river power stations have a production peak in summer. Storage power stations accumulate water during spring and early summer and produce throughout the year by properly managing the level of the storage lake.

Savelsberg et al. (2018) modelled the impact of climate change on the Swiss hydropower generation using the Swissmod model, which features a very detailed representation of 96% of the hydropower stations. More recently, the University of Basel calculated the changes in hydro inflows for the three RCP scenarios in CH2018 (2018) (see Marcucci et al. (2020) for a description of their calculation and results). They calculate the changes in the inflow for RoR, dams and pumped hydropower plants for the periods 2010–2039, 2040–2069 and 2070–2099. With these data we estimate the changes in the inflow from the average of the historical monthly generation pattern shown in Figure 2.3. Figure 2.4 presents the inflow for RoR and dams. The results show an important decrease in the inflow in the summer months (July, August and September) and an increase in winter (January, February and March) relative to the historical values.

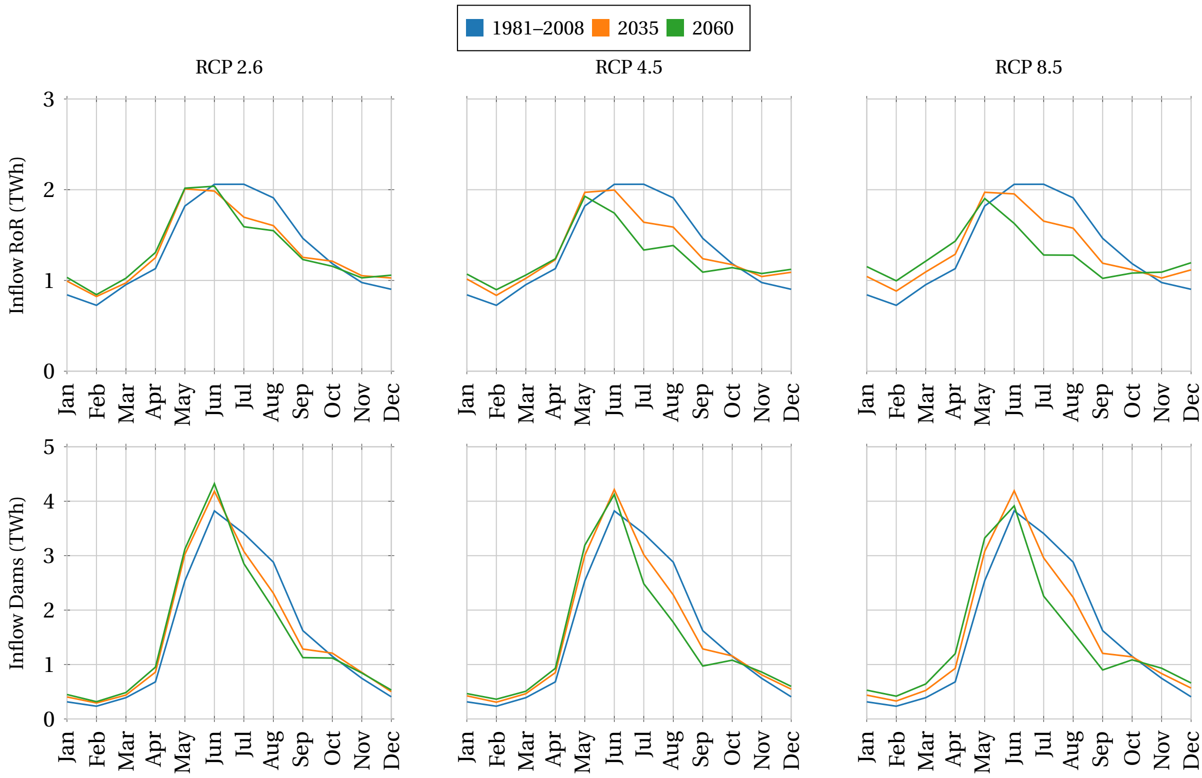

Figure 2.4: Hydropower monthly profile for the three RCP scenarios

Data available at https://data.sccer-jasm.ch/climate_hydro_inflows/

2.3 Photovoltaics

Photovoltaic (PV) electricity generation is expected to have the largest share of new renewables in the future Swiss electricity system. It has the obvious advantage of being less visually intrusive than wind generation. In order to properly understand the role that PV can play we need reasonable answers on the following three questions: (1) what is a realistic load factor for PV in Switzerland, i.e. what yearly output can be expected from a certain installed capacity? (Section 2.3.1), (2) How much PV capacity can be installed? (Section 2.3.2) (3) what is the yearly distribution of the solar irradiation? (Section 2.3.3)

2.3.1 Full load hours for solar photovoltaics in Switzerland

A PV installation consists of at least 2 parts: a module that delivers direct current (DC) power and an inverter that converts DC power into alternating current (AC) power that can be used directly or fed into the electricity grid.

When purchasing a PV installation, the first quantity of interest is the nameplate installed capacity, measured in $kW_{p,DC}$. This is the DC power that the module produces under Standard Test Conditions (STC), i.e. an irradiation of $1000\,W\,m^{-2}$, a module temperature of 25 °C, and an air mass of 1.5, conditions that are unlikely to be encountered in real operation. The ratio of DC power under STC conditions and the total irradiation onto the module ($1000\,W\,m^{-2}$ times the module surface) is the module efficiency at STC conditions. Today, a typical value for standard crystalline silicon modules is 15%. The specific investment costs are the ratio of investment costs and DC power, today in the range of 1000–2000 CHF/kW_p. In order to estimate the useful output, i.e. the AC power, a number of further effects have to be considered.

First of all, the DC power depends strongly on the module temperature (and to a lesser degree on the irradiation level). A module temperature of 25 °C is unlikely to be reached except in cold winter days. Every PV module comes with a Nominal Operating Cell Temperature (*NOCT*). The module reaches the NOCT under the following conditions: $800\,W\,m^{-2}$, 20 °C ambient temperature ($T_{ambient}$), $1\,m\,s^{-1}$ wind speed and a mounting with an open back side. A typical value for NOCT is 48–50 °C. The real module temperature (T_{module}) under other conditions can be estimated with this simple formula:

$$T_{module} = T_{ambient} + \frac{NOCT - 20}{800} I, \tag{2.3}$$

where I is the insolation level in $mW\,cm^{-2}$.

As a rule of thumb the loss in DC power is 0.4-0.5% for each degree that the module temperature is higher than the 25°C STC conditions. For a typical summer day at noon the ambient temperature may be 30°C, the module temperature can reach 58°C which results in a DC power loss of 13-16%.

Second, a number of losses occur before the DC power even reaches the inverter, e.g. soiling, shading, wiring, etc. The PVWatts(*R*) calculator uses a typical value of 14% (National Renewable Energy Laboratory).

The last element in the chain is the inverter itself. Two effects need to be considered: (1) the inverter may actually be undersized in capacity compared to the PV module itself. The reason is simply that the peak power production of the module is unlikely to occur often during the year, the inverter would therefore not be used efficiently. During maximum production, the PV module is therefore derated to not exceed the inverter power. This results in so-called clipping losses. The PV-to-inverter sizing ratio is typically 1.2–1.5. (2) The inverter itself has typical losses of 2–4%.

The cumulative AC output over the year (in kWh_{AC}) depends on the orientation of the PV installation and all loss mechanisms described above. The ratio of cumulative AC output to the installed nameplate DC capacity is measured in $kWh_{AC}/kW_{p,DC}$. The dimension of this ratio is hours and it represents the number of full load hours (FLH), i.e. the number of hours that the PV installation delivers the installed DC capacity. Using the PVWatts® calculator for the location of Geneva (National Renewable Energy Laboratory), we evaluated the FLH for six variants, combining two tilt angles (35 deg for a typical residential house and 10 deg for a PV module mounted on a flat roof, see Table 2.3) and three azimuth directions from south to west (there is little difference between east and west facing modules). As the table shows a typical value for the FLH in Switzerland is 900–1000 $kWh_{AC}/kW_{p,DC}$. The table shows also the capacity factor (η_{cap}), which results from dividing the FLH by 8760 h. Typical values in Switzerland will be $\eta_{cap} = 10 - 11\%$.

Table 2.3: Full load hours in Geneva

Tilt (°C)	35			10		
Direction	S	S/W	W	S	S/W	W
Full load hours ($kWh_{AC}/kW_{p,DC}$)	1051	997	850	998	980	932
Capacity factor (η_{cap},%)	12.0	11.4	9.7	11.4	11.2	10.6
Summer/winter ratio (−)	3.37	3.59	4.41	4.27	4.37	4.75

We use these FLH for the characterization of PV in the model. These numbers are confirmed by the latest statistics by SFOE (BFE, 2017b, SwissSolar, 2019, p. 52) (Table 2.4).

Table 2.4: Statistics 2014–2019 solar production in Switzerland (BFE, 2017b, SwissSolar, 2019, p. 52)

	2014	2015	2016	2017	2018	2019
Year-end installed capacity ($MW_{p,DC}$)	1060	1393	1664	1906	2173	2498
Yearly production (GWh/a)	841	1118	1333	1683	1945	2177
Full load hours ($kWh_{AC}/kW_{p,DC}$)	995	965	905	970	980	960
Capacity factor (η_{cap}, %)	11.4	11.0	10.3	11.1	11.2	11.0

2.3.2 PV potential in Switzerland

To model the possible contribution of PV to the future Swiss energy system we need to know the potential yearly generation (TWh/a) and its temporal distribution, especially the seasonal variation.

Walch et al. (2019) did an assessment of different studies to estimate rooftop PV potentials. They include the 6 studies in Table 2.5.

The BFE publised in April, 2019 (BFE, 2019c) a maximum potential for roof and facades in Switzerland of 67 TWh. We considered a maximum potential, slightly more conservative, of 50 TWh from Bauer et al. (2019).

2.3.3 Hourly profiles of solar irradiation in Switzerland

As discussed in the previous section, the temporal distribution of the solar energy is an important input to modelling the energy system. We represent the summer/winter ratios with the yearly hourly profiles of the solar radiation from the Institute for Solar Technology - HSR (Iturralde et al., 2019) (see Fig. 2.5).

Table 2.5: Solar potentials estimates from different studies, data from Walch et al. (2019, Table 2)

Study	Roof coverage (%)	Capacity factor (%)	Potential (TWh)
IEA (2002)	55%	10	15.0
Assouline et al. (2017)	60.5%	13.6	17.9
Assouline et al. (2018)	60.5%	13.6	16.3
Klauser (2016)	72.2%	13.6	53.1
Buffat et al. (2018)	70.1%	10.3	41.3
Walch et al. (2020)	56.4%	13.8%	25

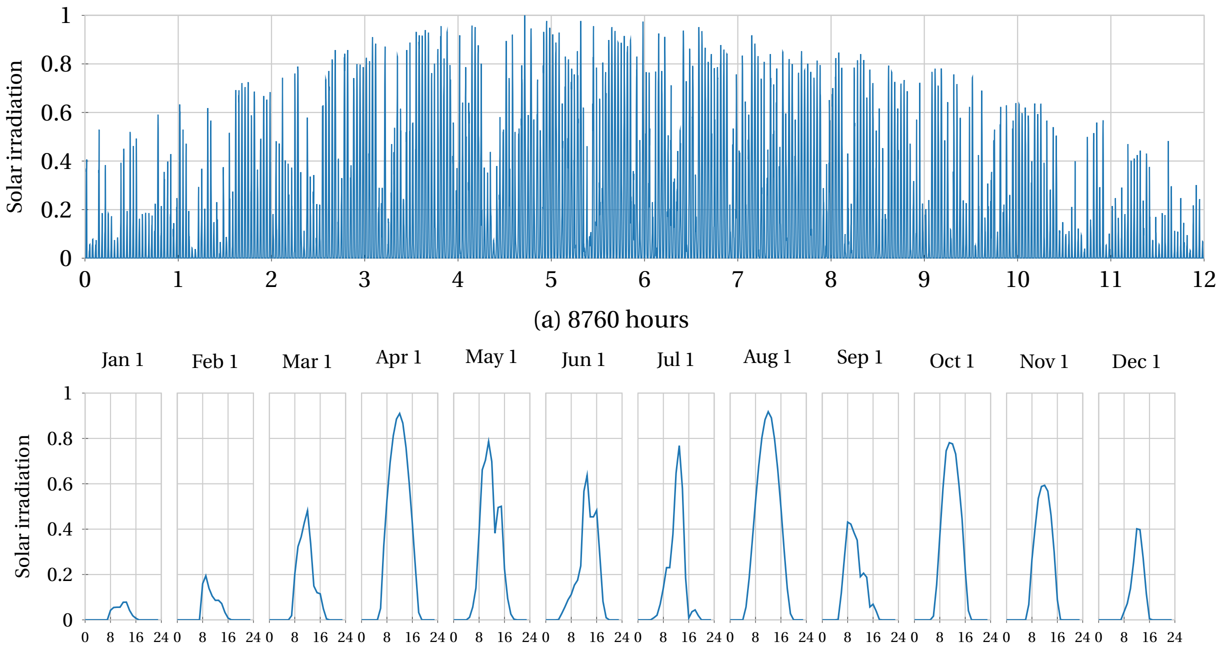

(a) 8760 hours

(b) First day of every month

Figure 2.5: Hourly profile for solar irradiation (normalized)

Data available at https://data.sccer-jasm.ch/renewable-hourly-profile-ses-eth/

2.4 Wind potential

Wind power could contribute to the future energy system as a complement to solar power, especially in those hours without sunshine. However, it has challenges for public acceptance given its impacts on landscape and noise. Table 2.6 summarizes the potentials calculated in different studies.

Our conservative potential is 1.7 TWh/a. It is based on the lower range of the potentials estimated by Cattin et al. (2012) that account for limits due to public acceptance and noise. Our progressive potential is 4.3 TWh/a based on the New Swiss wind energy concept (ARE, 2017). This potential is consistent with the assumptions in the Prognos (2012) Swiss Energy Strategy.

Table 2.6: Wind potentials estimates from different studies

	Potential (TWh)	
Study	**2035**	**2050**
Prognos (2012, Table 6-14)	1.7	4.2
Prognos (2012, Table 6-14) - Variant C	0.7	1.4
VSE (2012)	0.7–1.5	2–4
Cattin et al. (2012, p. 21)		
. Variants 1A and 2A (with noise restrictions)	-	2.7–4.5
. Variants 1B and 2B (with restrictions of noise and public acceptance)	-	1.7–2.2
ARE (2017)	-	4.3

2.4.1 Hourly profile for wind production in Switzerland

The temporal distribution of the wind energy is an important input to modelling the energy system. We represent the hourly distribution of the wind availability using the yearly hourly profiles of the wind speed from the original version of SES (Moret, 2017) (see Fig. 2.6).

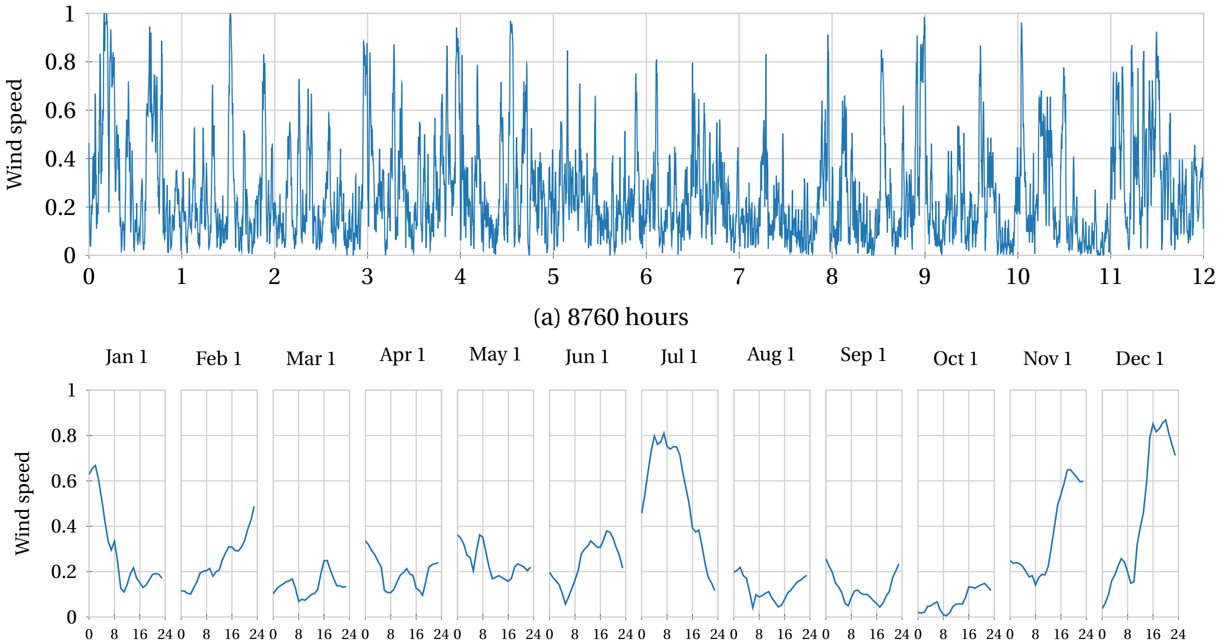

(a) 8760 hours

(b) First day of every month

Figure 2.6: Hourly profile for wind (normalized)

> Data available at https://data.sccer-jasm.ch/renewable-hourly-profile-ses-eth/

From this hourly profile we get a number of full load hours of 2010 h/a, which corresponds to a load factor of 2100/8760 = 23%. Therefore, our wind potential corresponds to an installed capacity of if we assume an average capacity per turbine of 3 MW and an average yearly load hours of 2000 h/a, the conservative potential requires around 315–380 wind turbines while the progressive potential 800–

950.

2.5 Imports of energy carriers

SES-ETH models the import of gas, oil, biofuels and hydrogen. We use the imports prices from the JASM project (Marcucci et al., 2020) (Table 2.7).

Table 2.7: Import price of energy carriers (CHF_{2010}/GJ): JASM variants (Marcucci et al., 2020)

	2017	2020	2030	2040	2050	2060	2020-2060	Reference
Oil								
Reference	9.6	8.8	18.5	20.7	22.8	24.7	2.61% p.a.	Reference Technology Scenario (IEA, 2017)
High	9.6	8.8	26	30.7	35.3	39.3	3.82% p.a.	JASM
Low	9.6	8.8	11	10.7	10.3	10	0.32% p.a.	Beyond 2DS Scenario (IEA, 2017)
Gas								
Reference	6.2	3.1	9.3	10.4	11	11.3	3.3% p.a.	Reference Technology Scenario (IEA, 2017)
High	6.2	3.1	11.2	13.8	15.5	16.5	4.27% p.a.	JASM
Low	6.2	3.1	7.4	6.9	6.5	6.2	1.76% p.a.	Beyond 2DS Scenario (IEA, 2017)
Biodiesel								
Reference	43.4	42.7	49.7	52.4	55	57.1	0.73% p.a.	FAO (2019) and Modern Jazz Scenario (WEC, 2019)
High	43.4	42.7	56.4	65.7	70.8	72	1.31% p.a.	Unfinsihed Symphony Scenario (WEC, 2019)
Low	43.4	42.7	41.4	40.1	40.1	40.1	-0.16% p.a.	JASM
Ethanol								
Reference	29.7	30.4	39.4	41.9	44.3	46.3	1.06% p.a.	FAO (2019), WEC (2019) and Brown et al. (2020)
High	29.7	30.4	48.2	59.2	64.1	67.4	2.01% p.a.	Unfinsihed Symphony Scenario (WEC, 2019)
Low	29.7	30.4	30.6	24.6	24.6	25.2	-0.46% p.a.	JASM
Hydrogen								
Reference	0	26.9	40.1	42.7	44.7	46.1	1.35% p.a.	IEA (2019)
High	0	26.9	41.6	44.4	52.1	59.8	2.02% p.a.	IEA (2019)
Low	0	26.9	38.5	41.1	37.3	32.3	0.46% p.a.	JASM

> Data available at https://data.sccer-jasm.ch/import-prices/

Chapter 3

Demand

This chapter describes the exogenous assumptions on end-use demands and the endogenous modelling of energy efficiency measures in the SES-ETH. Zooming-in Figure 1.1, we refer to the right part of the structure of the model (Figure 3.1).

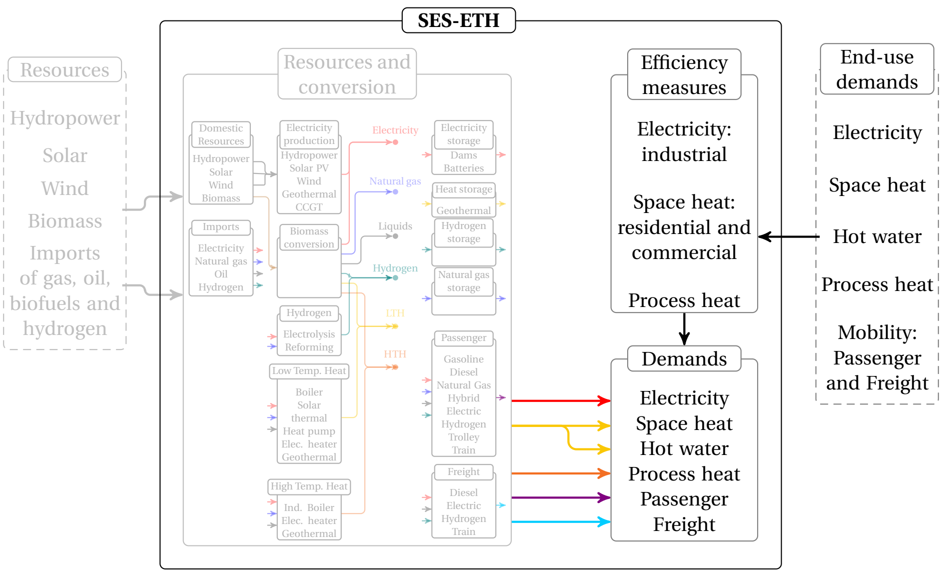

Figure 3.1: SES-ETH structure: Demand

In SES-ETH we modelled exogenous yearly demands for electricity, space heat, hot water, process heat and mobility. These demands are expressed in end-use demand. It is important to differentiate end-use demand from final energy consumption that is often used in energy statistics[1]. Final energy consumption is the amount of fuel needed to supply the end-use demand. For example, in the case of an oil boiler, final energy consumption is the amount of oil consumed by the boiler and end-use demand is the amount of heat produced by the boiler. Using end-use demands for our demand projections allow us to exclude the efficiency of the technology and to obtain the actual service demand.

Historically, space heating (mainly in the residential sector) and mobility are the end-uses with the largest share in the Swiss final energy demand (see Figure 3.2). In Swiss Energy Scope (SES) we consider demand for low temperature heat including space heating and warm water; high temperature process heat; electricity including lighting, cooling, cooking, appliances, information and communi-

[1] The yearly statistics of the BFE are all in units of final energy.

cations technologies (ICT) and motors; and mobility services for passengers and freight.

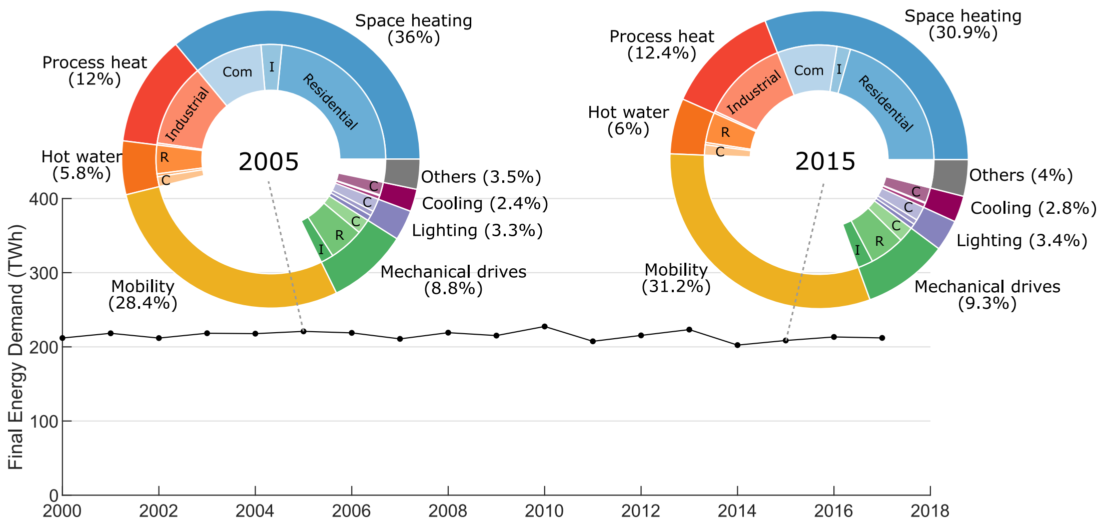

Figure 3.2: Historical Final Energy Demand. I: Industrial, R: Residential, C (or Com): Commercial (BFE, 2018, Tables 1, 15, 21 and 24)

SES-ETH uses time series (by year and hour) for all these demand categories. Each time series is decomposed in two parts: the total yearly demand and the hourly load profile. The two components are then multiplied to obtain the properly scaled time series.

The yearly demand for different energy services is known for the past and extrapolated into the future using the drivers presented in Table 3.1. We assume that each demand is proportional to one of the major drivers described in Marcucci et al. (2020): population, gross domestic product (GDP) or sectoral gross value added (GVA). However, the proportionality factor may not be constant over time. For example, estimating the demand for space heating depends on the energy reference area (ERA), the effective heated surface of the building that grows with either population or GVA, depending on the sector. In the same way, the demand for transport services –given in terms of person kilometers or ton kilometers– depends on GDP, population, and behaviour.

Table 3.1: Drivers of energy demands

Energy service	**Sector**			
	Residential	**Commercial**	**Industrial**	**Transport**
Space heating	$ERA_{res} = f(Pop)$	$ERA_{com} = f(Pop)$	$ERA_{ind} = f(GDP)$	
Warm water	Population	Population	GDP	
Process heat		GDP	GDP	
Lighting, cooling, cooking, appliances, ICT and motors	Population	GDP	GDP	
Mobility				GDP, population (based on ARE scenarios)

In SES-ETH we calculate the end-use demand for three different variants of the drivers: reference, low and high based on the assumptions in the JASM project (Marcucci et al., 2020). Table 3.2 presents the population and GDP.

Table 3.2: Macro-economic drivers: JASM Variants (Marcucci et al., 2020)

	2010	**2020**	**2030**	**2040**	**2050**	**2060**	**2010-2060**	**Reference**
Population (Million)								
Reference	7.86	8.68	9.42	10	10.43	10.79	0.63% p.a.	A-00-2020 (BFS, 2020)
High	7.86	8.68	9.63	10.53	11.34	12.12	0.87% p.a.	B-00-2020 (BFS, 2020)
Low	7.86	8.67	9.2	9.48	9.53	9.5	0.38% p.a.	C-00-2020 (BFS, 2020)
GDP ($BCHF_{2010}$)								
Reference	608.8	725.3	820.3	922.1	1022.9	1121.4	1.23% p.a.	SECO (2018)
High	608.8	725.3	850.5	984.5	1123.3	1268.9	1.48% p.a.	SECO (2018)
Low	608.8	725.3	794.9	867.7	931.4	984.6	0.97% p.a.	SECO (2018)

Data available at https://data.sccer-jasm.ch/macroeconomic-drivers/

3.1 Space heating demand

3.1.1 Energy Reference Area

The energy reference area (ERA) is the effective heated surface of a building. In SES-ETH, the historical ERA for the residential sector was calculated by Schluck et al. (2019). Schluck et al. (2019) used a comprehensive data set of the Swiss buildings stock with about 30,000 buildings and 23 descriptive features including construction period, building type, typology and canton. Table 3.3 presents the ERA in the residential, commercial and industrial sectors. Consistently with the Energy Statistics from the BFE (2018, p. 13), the ERA of the second homes and holiday houses is added to the commercial sector[2]. The occupancy factor (excluding second homes and holiday houses[3] from the total ERA) is 0.95, slightly higher than the 90% assumed by Jakob et al. (2016).

The ERA for the residential sector has been steadily growing over the past decades. This growth is linked to the increase in population but also to other trends such as smaller families and growing income. In the same way, the ERA for the commercial and industrial sectors has grown mainly due to economic growth. To extrapolate the residential ERA to the future, we assume an increasing ERA with population with a logarithmic function. This represents both limited space for living in Switzerland and decreasing marginal ERA to population. Figure 3.3 shows the ERA in the residential sector relative to population and the projected 2050 values in the reference, high and low variants. We use the same methodology for the commercial sector. In the industrial sector we use the GDP as the explanatory variable. The resulting ERA are shown in Table B.1. Figure B.1 shows the ERA per GDP, ERA per capita and total ERA for the three variants.

[2] All second homes are treated as holiday houses.

[3] Zweit- und Ferienwohnungen

Table 3.3: Historical Sectoral Energy Reference Area (Mm2)

	2000	2005	2010	2011	2012	2013	2014	2015	2016	2017
Residential sector										
BFE (2018, Tables 9 and 17)										
. With temporarily used buildings[a]	416	448	486	494	501	509	516	524	532	540
. Without temporarily used buildings	386	413	444	450	455	462	469	476	482	488
JASM from Schluck et al. (2019)										
. With temporarily used buildings									505	
. Without temporarily used buildings									482	
Commercial sector										
BFE (2018, Tables 9 and 17)[b]										
. Commercial sector	140	146	152	153	155	156	158	159	161	162
. Temporarily used buildings	31	34	43	44	46	47	48	49	50	52
. Total	170	180	194	197	201	203	205	208	211	214
Industrial sector										
BFE (2018, Table 9)[b]	83	84	87	88	88	89	90	91	91	92

[a] Second homes and holiday houses (*Zweit- und Ferienwohnungen*)
[b] Based on Wüest Partner (2019)

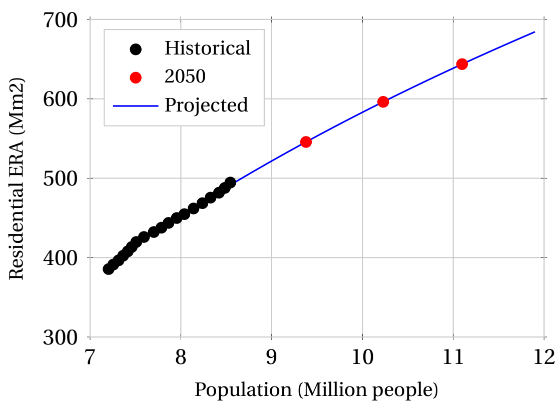

Figure 3.3: Historical and Projected (in red) residential ERA vs. Population

3.1.2 Building stock

The demand for space heating depends on development of the building stock. Starting from today's building stock we estimate the future building stock for single, multi family houses and commercial buildings.

Current building stock: Residential sector

We start with the building stock in 2017 (Schluck et al., 2019). Figure 3.4 shows the distribution of the ERA and the end-use demand by construction period and type. Houses built before 1945 account for 25% of the total ERA and 30% of the end-use demand. While those buildings built after 2001, account for 19% of the ERA and 11% of the demand. This is due to the significantly higher specific energy consumption of old buildings (Table 3.4).

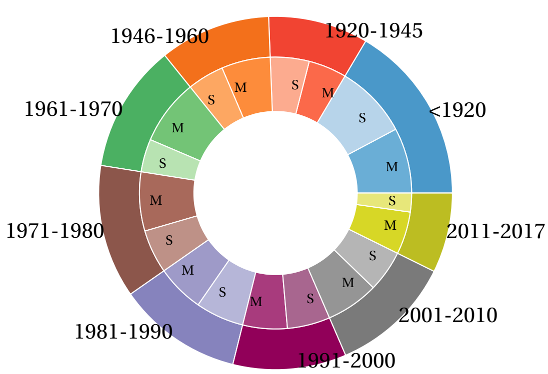

(a) Residential ERA by age and type

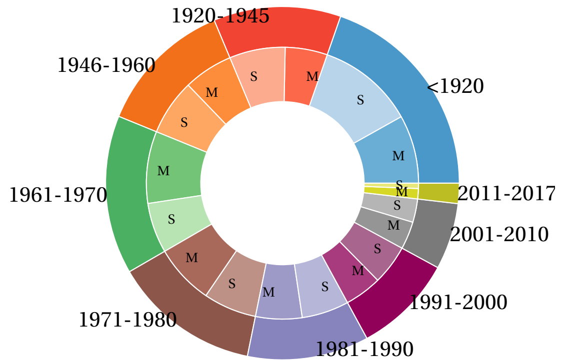

(b) Residential end-use energy demand by age and type

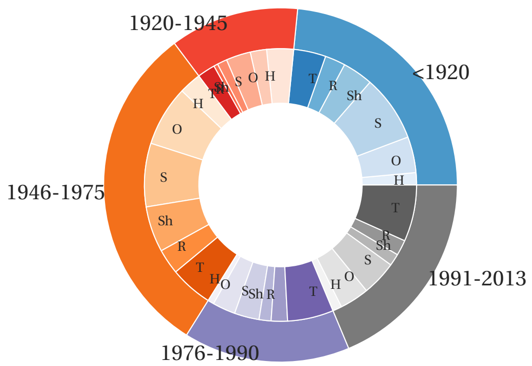

(c) Commercial ERA by age and type

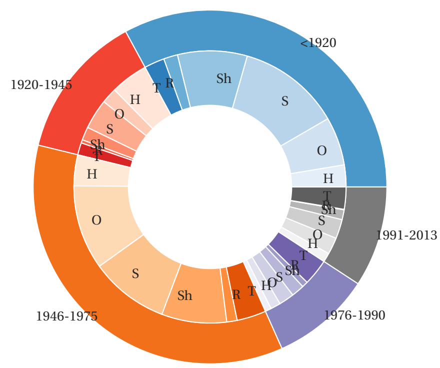

(d) Commercial end-use energy demand by age and type

Figure 3.4: 2017 building stock by age and type: Single family houses (S), multi-family houses (M), hospitals (H), offices (O), schools (S), shops (Sh), rest of commercial buildings (R) and temporarily used buildings (T)

Current building stock: Commercial sector

In the commercial sector, we start with the ERA by building type published by Wüest Partner (2019). We then use the distribution by age classes from Jakob et al. (2019, p. 68). The specific demand by age and building type was calculated by EMPA with the CESAR model (Streicher et al., 2020a). We added the temporarily used buildings, whose ERA we know from the BFE (2018), we assume that the distribution into age classes corresponds to that in the residential sector (see previous section). Finally, we also assume the total space heating demand for the temporarily used building from the BFE (2018) to be 8 PJ[4]. Figure 3.4 shows the distribution of the ERA and the end-use energy demand by construction period and type.

Future building stock

Following Müller (2006), Sandberg et al. (2016) and Sartori et al. (2016) we assume that the survival rate of the buildings follows a Weibull distribution. Hence the percentage of remaining buildings at time t follows the cumulative distribution function of the Weibull distribution, thus,

$$r(t) = \exp^{-\left(\frac{t-t_0}{\lambda}\right)^{\kappa}},$$

where λ and κ are the parameters that determine the kurtosis and skewness of the distribution (OECD, 2001). We use a $\kappa > 1$ to guarantee an S-shape. We use historical data and the share of historical buildings to estimate the parameter λ. The resulting survival rates for single, multi family houses and commercial buildings are shown in Figure 3.5. With the survival rates we can calculate the ERA by age category (Figure B.2 and Table B.2). Since the current building stock is the same for all marker scenarios, the only difference between them is for the buildings built after 2017.

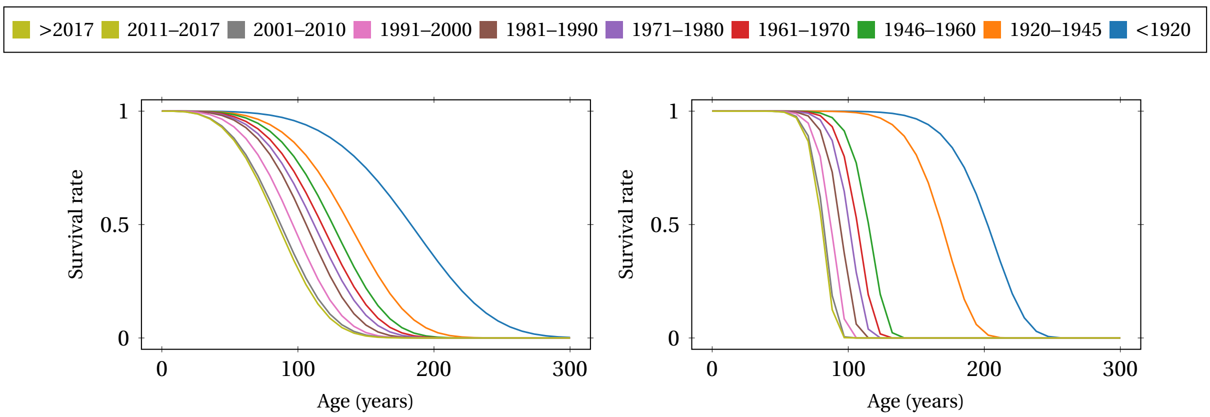

(a) Single family houses (b) Multi family houses and commercial buildings

Figure 3.5: Survival rate by age in the residential and commercial building stock

Specific energy demand

From Schluck et al. (2019) and Streicher et al. (2020a) we have the specific energy demands for the current building stock (without any renovation). For the future building stock we assume that the buildings will comply with current *minenergie* standards[5] with a specific energy demand that decreases with time as shown in Table 3.4.

[4] "Die Gesamtmenge, die vom Haushaltsbereich in den Dienstleistungssektor "verschoben" wird, liegt im Mittel der Jahre 2000 bis 2015 bei rund 14 PJ, davon sind rund 5.5 PJ Strom."

[5] Norm SIA 380/1

Table 3.4: Specific end-use energy demand by construction period (kWh/m2)

Construction period	SFH	MFH and commercial
<1920	92.9	77.3
1920-1945	104.3	81.3
1946-1960	110.1	73
1961-1970	109.1	78.4
1971-1980	89.7	72.9
1981-1990	76.1	72.4
1991-2000	75.2	60.2
2001-2010	62.5	47.3
2011-2017	44.4	29.4
>2017		
. 2020	40	35
. 2030	35	30
. 2040	30	25
. 2050	25	20
. 2060	20	15

Data available at https://data.sccer-jasm.ch/building-stock/

3.1.3 Climate correction

To determine the impact of the climate on the heating demand we use the change in Heating Degree Days (HDDs). We use the most common definition HDD 20/12: For every day at which the average temperature is below the heating limit $T_l = 12\,°\mathrm{C}$ we compute the difference of that temperature to an assumed building interior temperature $T_i = 20\,°\mathrm{C}$. Berger and Worlitschek (2019) calculated the future HDDs of the three climate scenarios in CH2018 (2018) using a GIS-based approach combining the spatial distribution of temperature (and therefore HDDs) and population. Figure 3.6 presents the median and the first and third quartiles of the HDD calculated by Berger and Worlitschek (2019).

We, therefore, compare the changes from the historical HDD to the projected values to estimate the correction factor for the demand. We use the average heating demand and HDD in the years 2014-2018 as starting baseline and correct the heating demand (that assumes a constant weather) with the corresponding projected HDD.

3.1.4 Demand before energy efficiency measures

Figure B.3 and Table B.3 present the evolution of the total space heating demand for a theoretical constant climate case and the three RCPs scenarios: RCP 2.6, RCP 4.5 and RCP 8.5 (Marcucci et al., 2020).

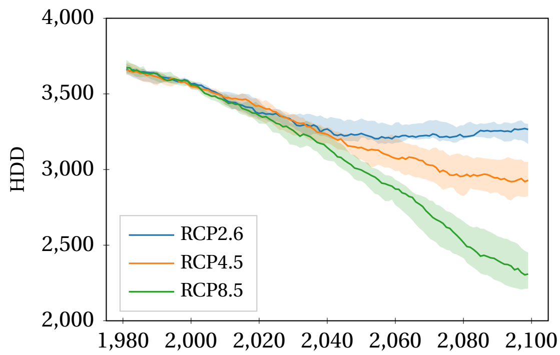

Figure 3.6: Heating degree days

Figure 3.7: Population weighted heating degree days in RCP 8.5, RCP 4.5 and RCP 2.6 (Berger and Worlitschek, 2019)

> Data available at https://data.sccer-jasm.ch/climate-data/

3.1.5 Energy efficiency measures

The amount of energy required to achieve the desired indoor temperature depends on the outside temperature, the energy reference area and also the insulation of the house. This includes, walls, windows, roof, and other parts of the building envelope. We use the results from Streicher et al. (2020a) and Marcucci et al. (2020, Chapter 4) to determine the energy efficiency curves in the SES-ETH model. For the residential sector, Streicher et al. (2020a) calculated the energy efficiency curves for 2016 using three different approaches of estimating the investment costs of the renovation measures. The first approach (full) includes all investment costs (related and not-related to energy efficiency improvements). The second approach (depreciation) accounts for the costs of the energy efficiency improvements plus a residual value to each building element. The third approach (improvement) accounts only for the cost of energy efficiency improvements. For the commercial sector, Streicher et al. (2020a) determine the energy efficiency curve for 2013. Since the estimations done by Streicher et al. (2020b) are for the residential building stock of 2016 and the commercial building stock of 2013, we need to estimate the energy efficiency curves for the future energy system. For that, we use the development of the building stock calculated in Section 3.1.2. To estimate the changes in the savings potentials we assume a constant specific energy saving (in kWh per m^2), so that when the ERA is reduced by 20% also the savings are reduced by 20%. Using the ERA by age category in Table B.1, we then obtained the following time dependent curves (Fig 3.8). These curves work just for a snapshot model and they represent the cumulative investments that need to be done from today until the corresponding year.

To use the energy efficiency curves in the SES-ETH we do a piecewise-linearization. We then use corresponding slopes as the specific costs in CHF/kWh (Figure 3.9). For the residential sector, we use the depreciation scenario since it discounts those costs not related to the energy system. The integration of these results into the SES-ETH model requires one last step: we model renovation measures as a virtual heat supply technology. This allows the model to choose the renovation level in competition with all the other supply technologies. We assume that the time series during the year of this technology corresponds to the difference between the time series of the non-retrofited and the fully retrofitted building. As described in Section 1.1, the investment costs for technologies are given in CHF/kW and not CHF/kWh. To calculate the investment costs from the specific costs in CHF/KWh,

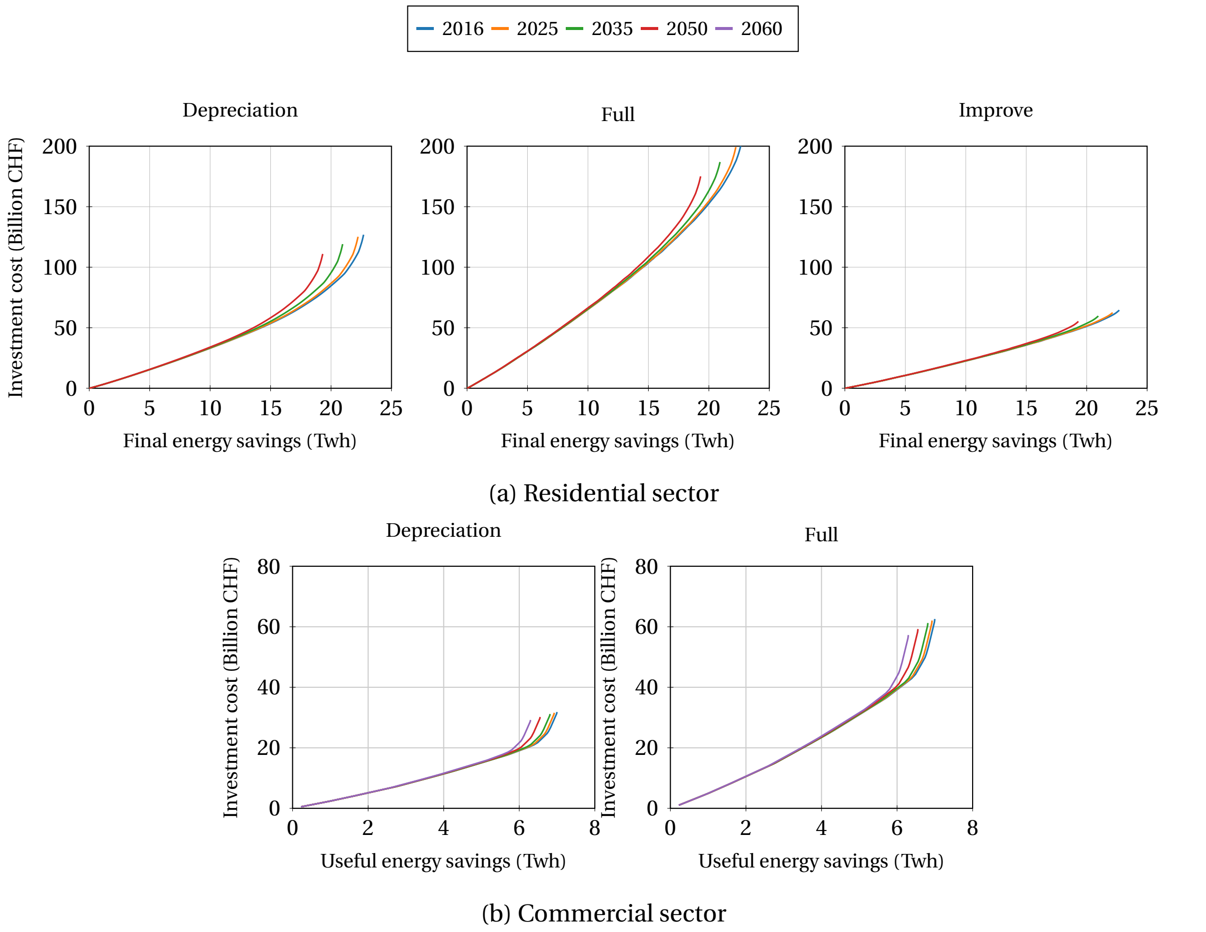

Figure 3.8: Projected Energy efficiency curves for different cost estimation scenarios. Based on Streicher et al. (2020b)

we need the number of full load hours for the virtual heat saving technology, i.e. the ratio of the total saved energy to the peak of the saving during the year. We assume a typical number of full load hours from middle Europe of 2000 full load hours per year; therefore, the 3.6 CHF/kWh in Figure 3.9 translate into 7200 CHF/kW.

3.2 Warm water

The drivers for the projection of warm water demand are population for the residential and commercial sectors and GDP for the industrial sector. Table B.4 and Figure B.4 present the resulting demand for the drivers in Table 3.2.

3.3 Process heat

Process heat is thermal energy supplied at a level higher than space heating of warm water. It is mostly used in specific industrial sectors with a small contribution in the commercial sector. We relate process heat demand to GDP. Table B.5 and Figure B.5 present the resulting demand for the drivers in Table 3.2.

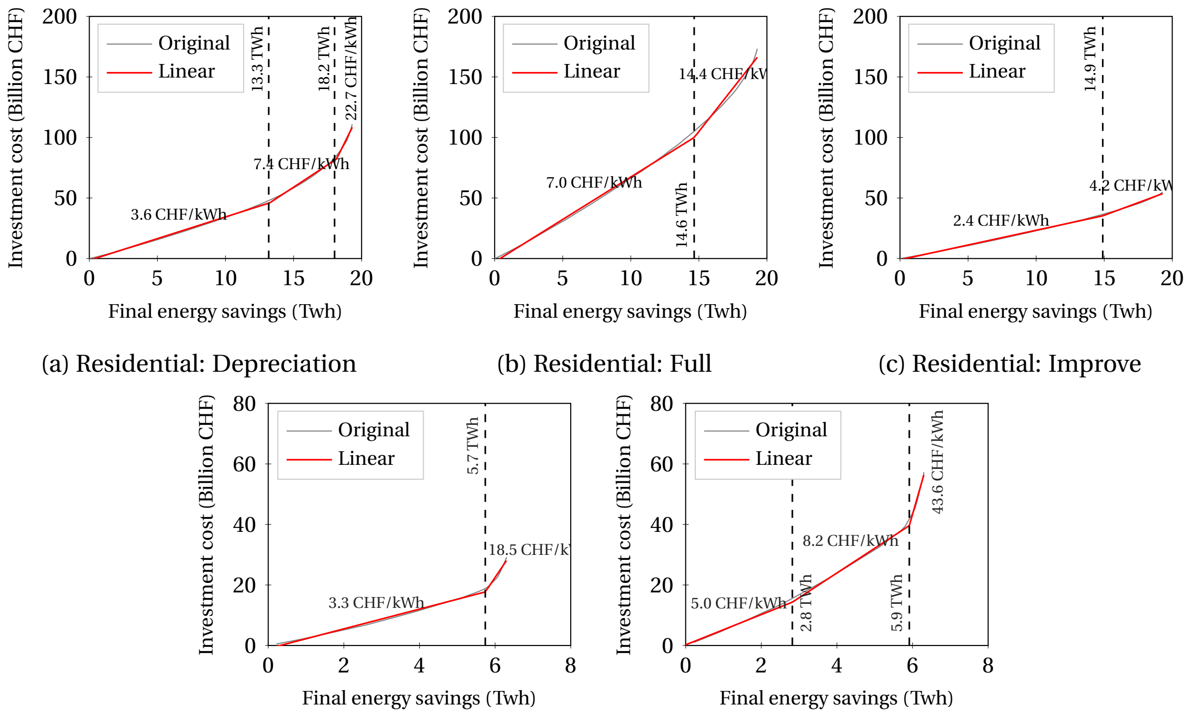

(a) Residential: Depreciation (b) Residential: Full (c) Residential: Improve

(d) Commercial: Depreciation (e) Commercial: Full

Figure 3.9: Linearized energy efficiency curves in 2060

3.3.1 Energy efficiency in industrial process heat demand

Zuberi et al. (2020) (based on Zuberi and Patel (2019), Zuberi et al. (2018, 2017), Zuberi and Patel (2017)) calculated energy potential savings and costs for improving energy efficiency in the production of process heat in the Swiss industry. The measures include various heat recovery options. Figure 3.10 presents the energy efficiency curves for process heat.

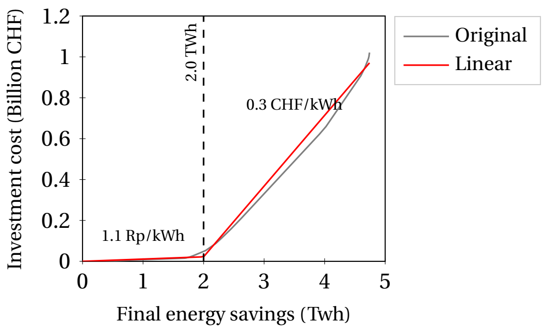

Figure 3.10: Energy efficiency cost curve for process heat. From Zuberi et al. (2020)

Data available at https://data.sccer-jasm.ch/energy-efficiency-industry/

3.4 Electricity: Electric appliances

In the electricity demand we include cooking, lighting, ICT, climate, processes (refrigerators, dishwashers, etc), electric motors, and air conditioning (A/C). The drivers used for the projections are population in the residential and commercial sectors and GDP in the commercial and industrial sectors. Table B.6 and Figure B.6 present the resulting demand for the drivers in Table 3.2.

3.4.1 Energy efficiency in industrial electricity demand

Zuberi et al. (2020) (based on Zuberi and Patel (2019), Zuberi et al. (2018, 2017), Zuberi and Patel (2017)) calculated energy potential savings and costs for electric motor systems in the Swiss industry. Figure 3.11 presents the energy efficiency curves for the use of electricity in the industrial sector.

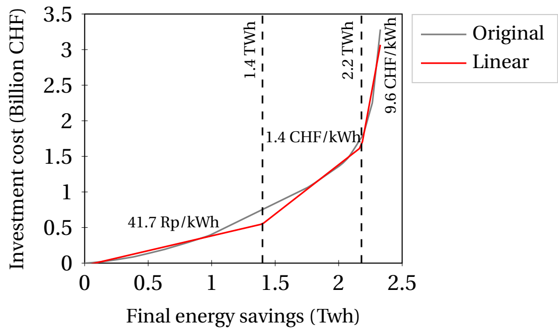

Figure 3.11: Energy efficiency cost curve for electricity in the industrial sector (Zuberi et al., 2020)

Data available at https://data.sccer-jasm.ch/energy-efficiency-industry/

3.5 Transport demand

The transport demand in SES-ETH is based on the Transport Outlook 2040 (ARE, 2016). These scenarios in this report include:

1. a reference scenario that extrapolates past developments of spatial planning and transport policies using medium projections of population and GDP;
2. scenarios assuming higher and lower population and GDP growth;
3. and scenarios with alternative spatial planning and transport policies:
    - Balance: integrates aspects of sustainability (e. g. densification) and prioritizes public transport.
    - Sprawl: more pronounced urban sprawl and gives precedence to individual mobility.
    - Focus: differentiates more sharply between urban and rural areas, with an emphasis on urbanization. Transport growth occurs mainly in and between cities.

To calculate the three variants of the transport demand in SES-ETH, we use the historical data from the BFS (2019b,c,a) and the ARE growth rates in the reference, high and low variants. The Balance, Sprawl and Focus scenarios are within the range of high and low population. For the projections after 2040, we assume a decreasing growth rate in the demand per capita and the demand per GDP for the passenger and freight demand, respectively.

Figure B.7 and Tables B.8 and B.7 present the passenger and freight transport projections from the different scenarios.

3.6 Hourly profiles

The original version of Swiss Energyscope (Moret, 2017) had a monthly time resolution. This allowed us to model the seasonal effects but neglects the intra-day variation. SES-ETH models the demand with a time series (by year and hour) for all the demand categories in Table 3.1. Each time series is decomposed in two parts: the total yearly demand (described in the previous sections) and the hourly load profile. The two components are then multiplied to obtain a properly scaled time series.

3.6.1 Space heat

The demand for space heating is rarely measured on an hourly scale, we therefore rely on simulation results. These have been done for multi- and single-family houses, both for old and new buildings (see Iturralde et al. (2019)). The resulting hourly time series represent the instantaneous power of the heat delivery system, e.g. a radiant floor delivered for actual buildings. Figure 3.12 depicts the normalized hourly profiles for the four archetypes (single and multi family houses, old and new).

3.6.2 Warm water

Yilmaz et al. (2020) calculated the hourly profile in Figure 3.13. We depict only the first day of each month because the seasonal changes are less relevant than the daily ones.

3.6.3 Process heat

The hourly profiles for process heat are based on the typical days from PSI[6]. The data distinguishes weekdays and weekends, as well as winter, intermediate and summer seasons. We mapped those typical days to hour yearly profile in Figure 3.14.

3.6.4 Electricity

Yilmaz et al. (2020) calculated the hourly profile for the electricity demand shown in Figure 3.15.

3.6.5 Cooling

Yilmaz et al. (2020) used the CESAR model to calculate the hourly profile for cooling demand shown in Figure 3.16.

[6]Data available at https://data.sccer-jasm.ch/demand-hourly-profile/

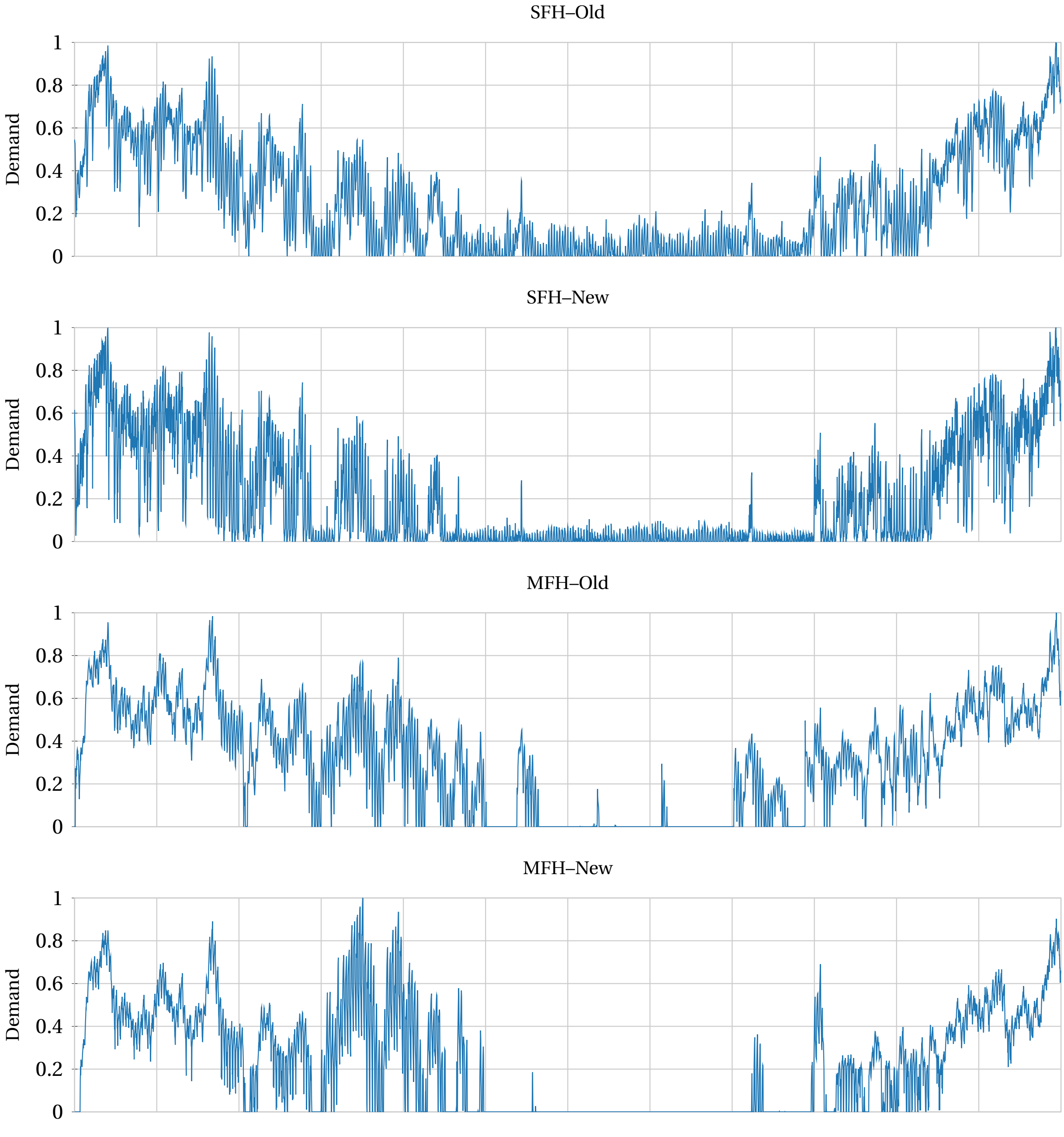

Figure 3.12: Hourly profile space heating (normalized)

Data available at https://data.sccer-jasm.ch/demand-hourly-profile-hsr/

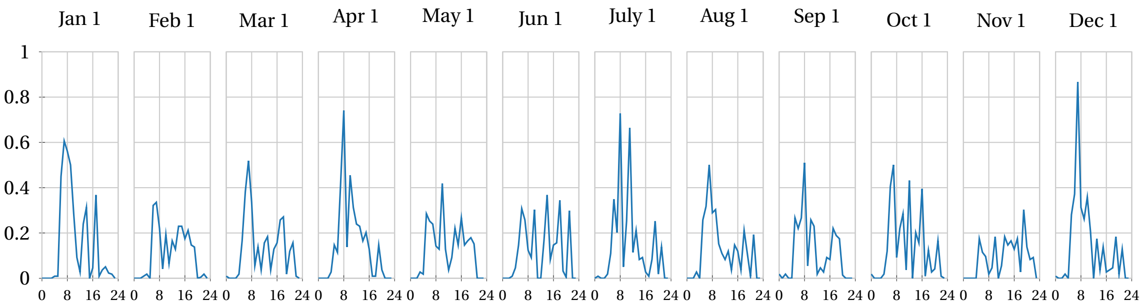

Figure 3.13: Hourly profile warm water for selected days

Data available at https://data.sccer-jasm.ch/demand-hourly-profile-retrofits-cesar/

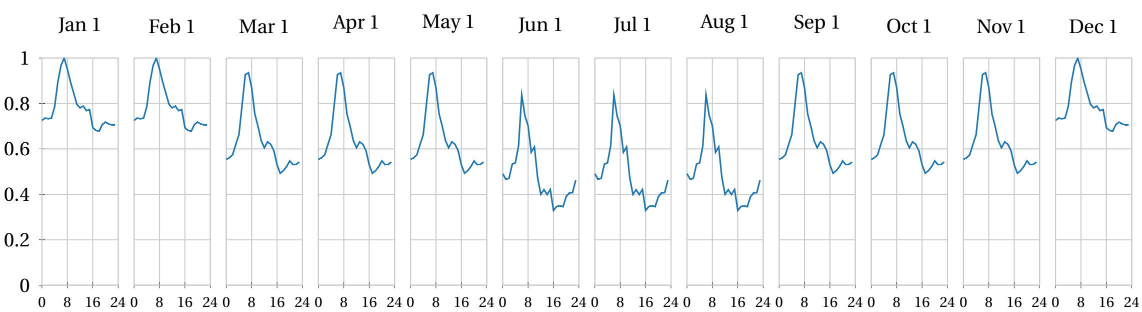

Figure 3.14: Hourly profile process heat for selected days

Data available at https://data.sccer-jasm.ch/demand-hourly-profile/

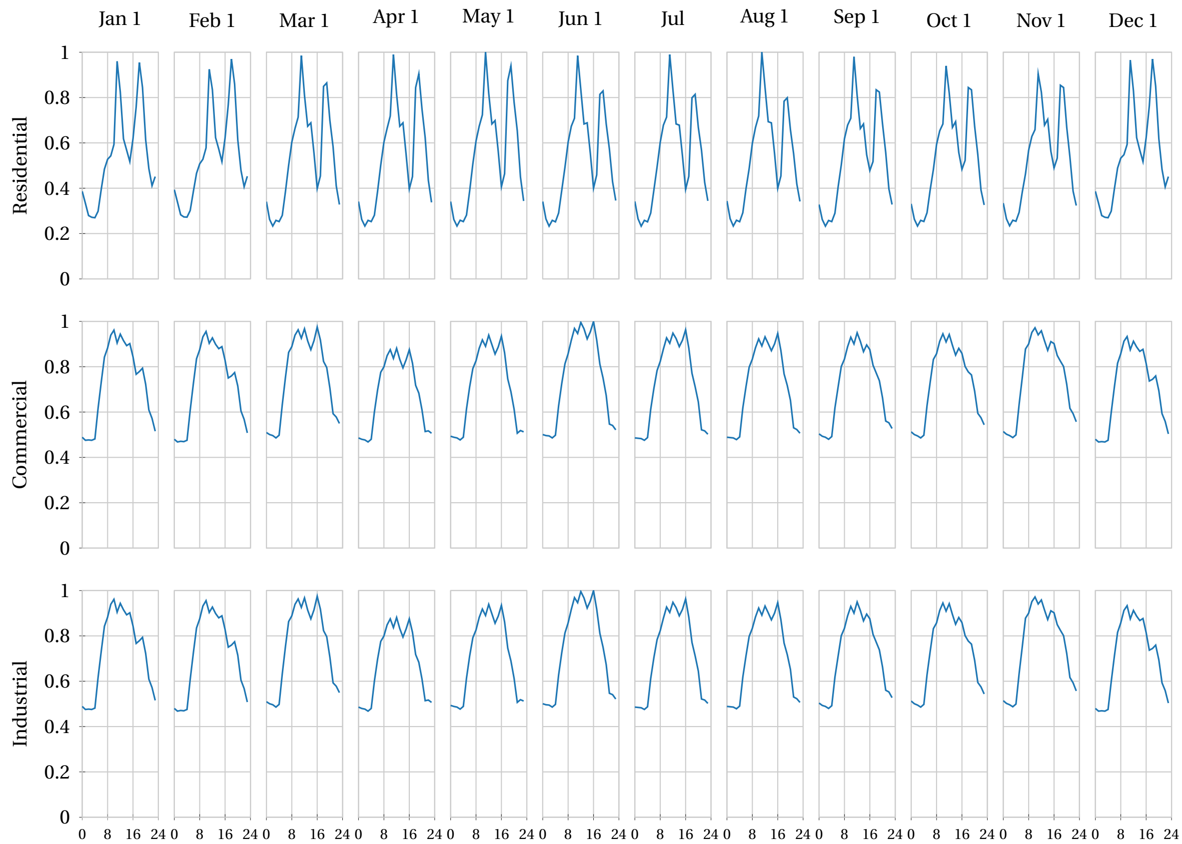

Figure 3.15: Hourly profile electricity for selected days

Data available at https://data.sccer-jasm.ch/household-daily-load-curves/

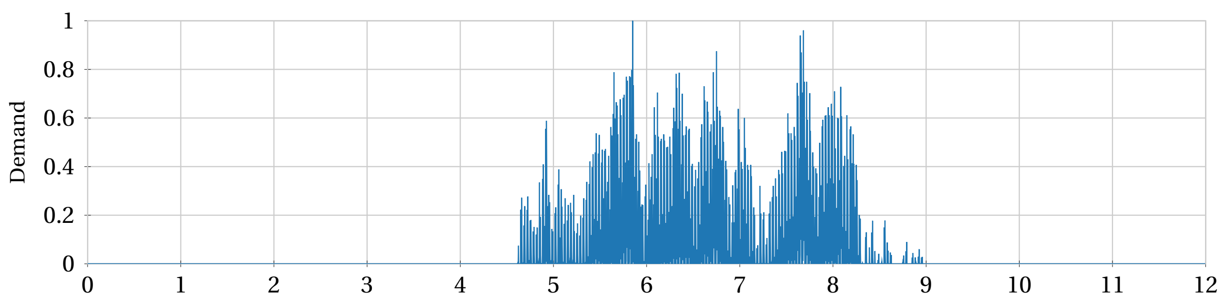

Figure 3.16: Hourly profile cooling

Data available at https://data.sccer-jasm.ch/demand-hourly-profile-retrofits-cesar/

Chapter 4

Technologies

This chapter describes the technologies included in the SES-ETH. Zooming in Figure 1.1, we refer to the middle part of the structure of the model (Figure 4.1).

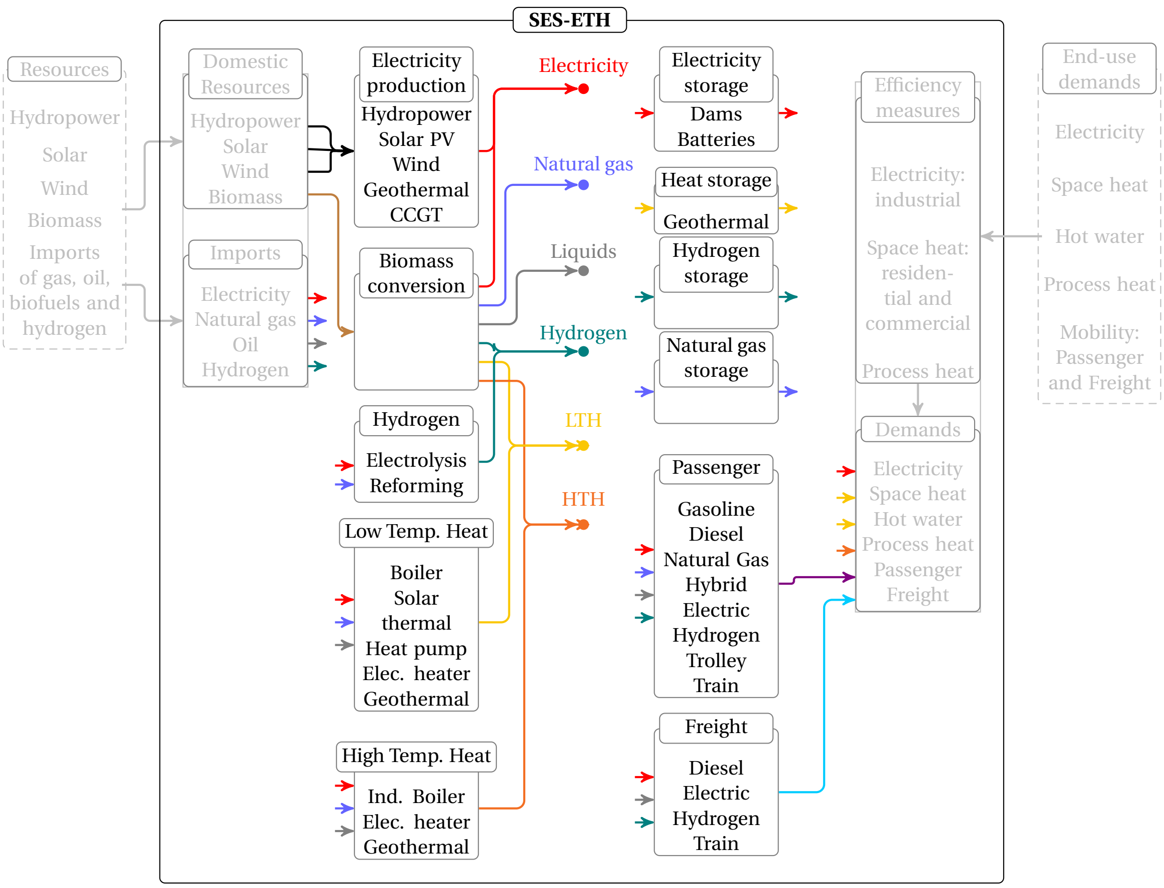

Figure 4.1: SES-ETH structure: Technologies

4.1 Technologies for electricity, heat and hydrogen production

In SES-ETH we include technologies for electricity production, heat production, combined heat and power and hydrogen production. We include technologies using renewable resources, fossil fuels gas and hydrogen. Table 4.1 shows the different technologies, their investments costs and efficiency.

Table 4.1: Electricity, heat and hydrogen technologies

Technology	Fuel	Inv. cost (CHF/kW)			Efficiency (%)					Reference
		Ref	Low	High	Ele	HTH	MTH	LTH	H_2	
Electricity production (cost per kWe)										
Solar PV		1000	500	1500						Bauer et al. (2017, 10kW, p. 47)
Wind		2000								Bauer et al. (2017, p. 294)
Hydro Dams		6000								Bauer et al. (2017, Hydro general, p. 44)
Hydro Run of River		6800								Bauer et al. (2017, p. 45)
Geothermal		10000								Bauer et al. (2017, 5.5 MW including plant and well, p. 469)
Gas combined cycle	CH4	900			60					Bauer et al. (2017, p. 650)
. With CCS		1509			54					Bauer et al. (2017, p. 651)
Hydrogen combined cycle	Hydrogen	900			63					JASM assumption: same cost as CCGT
Waste combined cycle	Waste	6000	5000	7000	33					Bauer et al. (2017, Existing KVA in Switzerland, p. 444 - last column)
. With CCS		7800	6800	8800	25					SES-ETH assumption
Wood combined cycle	Wood	6000	5000	7000	33					Bauer et al. (2017, p. 444 - last column)
. With CCS		8160	7160	9160	24					SES-ETH assumption
Combined heat and power (cost per kWth)										
Gas industrial CHP	CH4	765			44		42			Bauer et al. (2017, 1MW, p. 653)
Gas medium size CHP	CH4	1260			40			47		Bauer et al. (2017, 0.1MW, p. 653)
Hydrogen industrial CHP	Hydrogen	765			44		42			SES-ETH assumption: same cost as gas
Hydrogen medium size CHP	Hydrogen	1260			40			47		SES-ETH assumption: same cost as gas
Sewage sludge CHP	Sewage sludge	2143	1600	2600	20		56			SES-ETH assumption: same cost as waste
Biogas medium size CHP (Including biogas production from Manure with eff. 37%)	Manure	6000			12			19		
Wood industrial CHP	Wood	900	500	1300	26		54			Keppo and Savola (2007)
Wood medium size CHP	Wood	1158			24			56		

Table 4.1: Electricity, heat and hydrogen technologies (continued)

Technology	Fuel	Inv. cost (CHF/kW)			Efficiency (%)					Reference
		Ref	Low	High	Ele	HTH	MTH	LTH	H_2	
Waste industrial CHP	Waste	2069	1600	2600	20		58			Bauer et al. (2017, Existing KVA in Switzerland, p. 444 - last column)
Waste medium size CHP	Waste	2069			20			58		Bauer et al. (2017, Existing KVA in Switzerland, p. 444 - last column)
. With CCS		3093			17			40		
Heat production (cost per kWth)										
Gas industrial boiler	CH4	90				70				Radov et al. (2009, p. 91)
Gas medium size boiler	CH4	150						80		Radov et al. (2009, p. 91)
Gas decentralized boiler	CH4	1000						80		SES-ETH assumption
Oil industrial boiler	Oil	80				70				SES-ETH assumption: 90% of gas cost
Oil medium size boiler	Oil	130						80		SES-ETH assumption: 90% of gas cost
Oil decentralized boiler	Oil	900						80		SES-ETH assumption: 90% of gas cost
Hydrogen industrial boiler	Hydrogen	90				70				SES-ETH assumption: same cost as gas
Hydrogen medium size boiler	Hydrogen	150						80		SES-ETH assumption: same cost as gas
Wood industrial boiler	Wood	650	500	800		80				Radov et al. (2009, p. 83)
Wood medium size boiler	Wood	950						80		Radov et al. (2009, p. 83)
Wood decentralized boiler	Wood	2000						80		Radov et al. (2009, p. 83)
Waste industrial boiler	Waste	650	500	800		75				SES-ETH assumption: same cost as wood
Sewage sludge industrial boiler	Sewage sludge	800	600	1000		70				
Electric industrial boiler	Electricity	275				95	95			Radov et al. (2009, p. 93)
Electric medium size boiler	Electricity	325						95		Radov et al. (2009, p. 93)
Electric decentralized boiler	Electricity	650						95		Radov et al. (2009, p. 93)
Water source heat pump - Medium size	Electricity	2000						400		
Water source heat pump - Decentralized	Electricity	2300	1300	3300				400		
Ground source heat pump - Decentralized	Electricity	2600	1700	3600				400		Radov et al. (2009, p. 79)
Air source heat pump	Electricity	2100	1200	3000				300		Radov et al. (2009, p. 75)
Solar thermal medium size		600	500	750						

Table 4.1: Electricity, heat and hydrogen technologies (continued)

Technology	Fuel	Inv. cost (CHF/kW)			Efficiency (%)					Reference
		Ref	Low	High	Ele	HTH	MTH	LTH	H_2	
Solar thermal decentralized		1500	1200	1700						
Deep geothermal industrial		3000	2000	4000						
Deep geothermal medium size		3000	2000	4000						
Hydrogen production (cost per kW H_2)										
Electrolysis	Electricity	1000	600	1500					70	Christensen (2020), IEA (2019)
Steam methane reforming (with CCS)	Natural Gas	1500	1000	2000					77	IEA (2019, Reforming with CCS, Assumptions, p. 3)
Autothermal reforming	Natural Gas	1500	1000	2000					77	JASM assumption: Same as steam reforming

Data available at https://data.sccer-jasm.ch/energy-conversion-technologies-ses-eth

4.2 Biomass conversion routes

Biomass is a special resource that can be used for the production of electricity, heat, and other fuels including methane, hydrogen and liquid biofuels. Therefore, we model in detail some of the most relevant conversion routes in SES-ETH. Figure 4.2 presents the different technology pathways for biomass (based on the JASM-Biosweet (Guidati et al., 2020)). It shows the routes that are currently implemented in the model, which excludes those that are less likely to be realized from the entire set of conversion pathways described in Guidati et al. (2020).

Wood can be used in direct combustion (7a) and gasification (5a). Wood combustion (7a) produces heat at different temperatures. Low temperature heat can be used for domestic uses and high temperatures for industrial purposes. Wood can also be combusted to drive a power cycle producing electricity and heat (7b). An alternative route is wood gasification (5a). Here the basic constituents of wood (carbon, hydrogen and oxygen) are recombined in the presence of an oxidant (air or oxygen) to produce a syngas composed of carbon monoxide, hydrogen, CO_2 and other species. This syngas can be subsequently processed to synthetic natural gas (via a methanation reaction, 5b and 5g) or hydrogen (via a water gas shift reaction, 5d). Alternatively, the syngas may be combusted in a gas motor or a gas turbine combined cycle to produce electricity and heat (5d).

Manure can be used in anaerobic digestion (6a) that produce raw biogas, a mixture that usually contains around 40-60% methane and the rest is mostly CO_2. Today, in Switzerland, the biogas produced from anerobic digestion is used mostly in small internal combustion engines to produce electricity and heat. The latter is used on-site as much as needed and the rest is discarded. A future energy system may profit from another route, namely an upgrading of the raw biogas (6b) to biomethane (by separating CO_2 and other species), which can then be injected into the natural gas grid. This gas

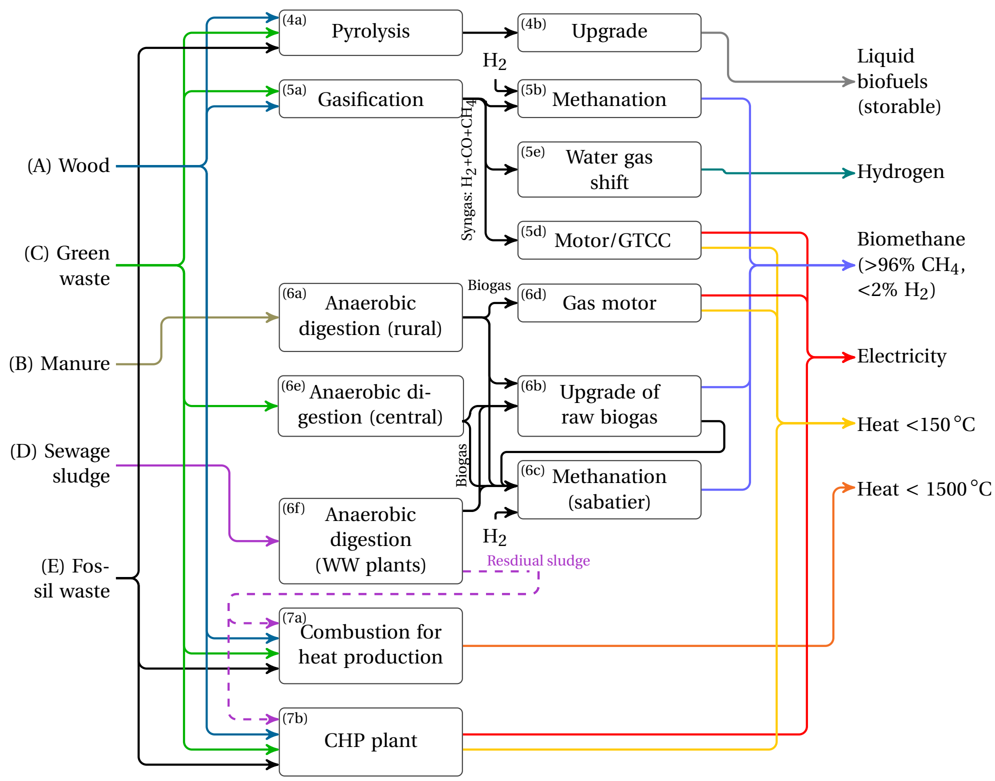

Figure 4.2: Mapping of Biomass Technologies and Resources

may then be used for a variety of processes, including seasonal storage in neighboring countries such as Germany or France. The separated CO_2 may be further combined with hydrogen from electrolysis to produce additional methane via a Methanation (Sabatier) reaction (6c). Such an alternative route is hindered by the fact that the average farm size in Switzerland is very small. As shown in the report by WSL (Thees et al., 2017), even a reasonable amount of electricity production via the first route requires already a collection of manure within a 1 km range. All subsequent steps such as biogas cleaning, electrolysis or methanation would require an even larger size to be technically feasible and profitable.

Green waste can be used in central anerobic digestors (6e) and combustion plants (7b) and (7c).

Concerning sewage sludge, current Swiss regulations enforce the energetic use of sewage sludge from waste water treatment plants (WW, *Abwasser-Reinigungsanlagen*) with a cascade utilization (Thees et al., 2017, p. 279ff). The fresh sewage sludge undergoes goes first to an anaerobic digestor (6f) that produces biogas, which can be used on-site or injected into the gas grid after gas cleaning. The residual sludge is then combusted in waste incineration plants, specialized sludge incinerators and cement plants.

The detailed description of the different conversion processes can be found in the JASM-Biosweet report (Guidati et al., 2020).

Table 4.2 presents the characteristics of some of the technologies in Figure 4.2 (we include the characteristics of all technologies using biomass resources for the production of electricity in Table 4.1).

Table 4.2: Biomass and hydrogen technologies (Guidati et al., 2020)

	Technology	Feedstock	Product	Inv. cost (CHF/kW)			Eff (%)	Elec. use (MWhel/ MWh)	Reference
				Ref	Low	High			
(4)	Pyrolysis	Wood	Liquid biofuel	2600			67	0	Brown et al. (2020)
(5a) + (5b)	Gasification + methanation	Wood	Methane	2900	2300	3500	63	0	Schildhauer (2018)
(5a) + (5e)	Gasification to H2 (dual fluidized bed)	Wood	Hydrogen	2000	1500	2500	62	0.11	NREL (2011)
	. With CCS	Wood	Hydrogen	2300	1800	2800	62	0.21	
(5a) + (5e)	Gasification to H2 (sorption enhanced reforming)	Wood	Hydrogen	2000	1500	2500	71	0.18	NREL (2011)
	. With CCS	Wood	Hydrogen	2300	1800	2800	71	0.28	
(5a) + (5e)	Gasification to H2 (entrained flow)	Wood	Hydrogen	2000	1500	2500	66	-0.11	NREL (2011)
	. With CCS	Wood	Hydrogen	2300	1800	2800	66	0.03	
(6a) + (6b)	Anaerobic digestion (rural)	Manure	Methane	1200			37	0	Ro et al. (2007)
(6e) + (6b)	Anaerobic digestion (central)	Green waste	Methane	1200			37	0	Ro et al. (2007)
(6f) + (6b)	Anaerobic digestion (waste water treatment)	Sewage sludge	Methane	1200			54	0	Ro et al. (2007)
(6c)	Methanation (Sabatier)	Biogas (55% CH4, 45% CO2) + H2	Methane	900	800	1000	83	0.01	Witte et al. (2018)

Data available at https://data.sccer-jasm.ch/biomass-conversion-technologies/ and https://data.sccer-jasm.ch/energy-conversion-technologies-ses-eth

Chapter 5

Uncertainty analysis

We consider external factors that are not as sensitive to domestic policies or individual behavior change changes (such as population and economic growth, global climate change, and technology characteristics) independent from the scenario definition and analyze them as uncertain factors with probability distributions.

Our approach is distinct from other modeling and scenario efforts in that we create envelopes of robust results. The results will reveal trends and drivers we face in optimizing the Swiss energy system under different policy regimes. These trends and drivers are more informative than point-estimates alone: In comparing the set of results, we can identify the developments in the energy system that are more or less fixed—that are common to all the scenario results—and those that vary significantly. For instance, given the recent price developments of solar panels, our models will likely select them to be part of the future energy system while other technologies with less favorable economics, such as hydrogen or domestic liquid biofuels, might only be selected in special cases where they are competitive.

5.1 Approach

We model our exogenous assumptions about the state-of-the-world as uncertain independent parameters with different probability distributions. These assumptions include: (1) Population and GDP (GDP is calculated based on the population projection); (2) global climate change; and (3) technology characteristics.

We construct our set of scenarios using a Quasi-Monte Carlo method with a Sobol sequence[1]. The set of n scenarios of dimension, d, (Population, climate and technology costs) is defined with a $d \times n$-Sobol sequence. The sequence gives us n tuples of dimension d. Each dimension has a uniform distribution $U(0,1)$ of realizations (e.g., future populations) that we then transform into the distribution of the corresponding variable. The result is a set of n tuples of the form: (pop_1, climate_1, cost_1, $\ldots$, $y_{1,d}$) ,$\ldots$, (pop_n, climate_n, cost_n, $\ldots$, $y_{n,d}$). Each tuple corresponds to the exogenous assumption in one of our scenarios (Fig. 5.1).

[1] A Sobol sequence is a quasirandom, or low discrepancy, sequence that samples the input space in a more uniform way than a random sequence (Niederreiter, 1992). This has the advantage of covering the entire space with fewer scenarios than a random sampling method would.

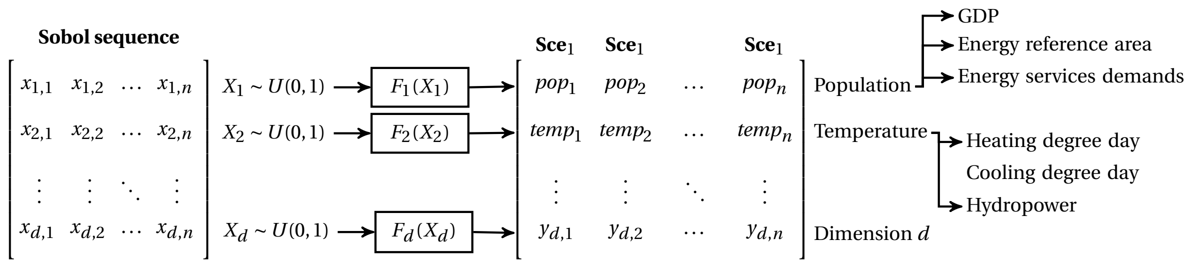

Figure 5.1: Input assumptions from Sobol Sequence

5.2 Stochastic variables

5.2.1 Population

We use the three variants from the JASM drivers and assume the population is uniformly distributed between the low and high variants (Table 3.2). The first dimension from the Sobol sequence give us a uniform distribution $\sim U(0,1)$ that we then scale with the minimum and maximum.

For the following variables we use the population as the driver to determine their future evolution:

1. Gross domestic product: The GDP projections depend on the population projections. We use the same methodology used by the SECO (2018) to estimate GDP for each of our population variants.

2. Biomass and waste resources: We estimate the potential for some of the biomass and waste categories based on either population of GDP growth, following the methodology described in the JASM-Biosweet report (Guidati et al., 2020). These biomass categories are:

Category	Driver
Waste wood	Population
Sewage sludge	Population
Municipal waste	Population
Other waste fraction (construction, special waste)	GDP

3. Energy demands: We estimate all end-use demands using either population or GDP as drivers (as shown in Table 3.1).

5.2.2 Global climate change

Future climate change is an uncertain variable that depends on global economic development and mitigation actions. We use a discrete distribution of the three RCP scenarios (CH2018, 2018) as three possible realizations of the future temperature increase. Based on the climate change scenario we calculate: (1) The climate correction for heating and cooling demands as described in section 3.1.3; and (2) The yearly distribution of available hydro inflow for hydropower plants as shown in section 2.2.2.

5.2.3 Investment costs of technologies and fuel costs

We consider the investment costs of certain technologies including solar PV, heat pumps, geothermal, electric vehicles, sabatier reactors, gasifiers and storage technologies stochastic in the mode (this is a summary of the investment costs in Table 4.1). We use the same approach for some fuel costs.

Technology	Cost
Electricity production (CHF/kWe)	
Solar PV	500–1500
Waste combined cycle Waste	5000–7000
. With CCS	6800–8800
Wood combined cycle	5000–7000
. With CCS	7160–9160
Combined heat and power (CHF/kWth)	
Sewage sludge CHP	1600–2600
Wood industrial CHP	500–1300
Waste industrial CHP	1600–2600
Heat production (CHF/kWth)	
Wood industrial boiler	500–800
Waste industrial boiler	500–800
Sewage sludge industrial boiler	600–1000
Water source heat pump - Decentralized	1300–3300
Ground source heat pump - Decentralized	1700–3600
Air source heat pump	1200–3000
Solar thermal - medium size	500–750
Solar thermal decentralized	1200–1700
Deep geothermal industrial	2000–4000
Deep geothermal medium size	2000–4000
Hydrogen production (CHF/kWH2)	
Electrolysis Electricity	600–1500
Steam methane reforming (with CCS)	1000–2000
Autothermal reforming	1000–2000
Biomass conversion (CHF/kW)	
Wood gasification + methanation	2300–3500
Wood gasification to H2	1500–2500
. with CCS	1800–2800
Methanation (sabatier)	800–1000
Fuel prices (CHF/kWh)	
Gas import	s 0.03–0.04
Biogas imports	0.1–0.2
Hydrogen imports	0.1–0.2
Domestic wood	0.04–0.08

5.3 Typical results from the uncertainty analysis

Using the uncertainty analysis, we can analyze different scenarios of the future Swiss energy system. Figure 5.2 shows typical results of this approach. The Monte Carlo variation of uncertain drivers is represented by showing the median (the white dash), the interquartile range (the colored box) and the minimum and maximum (the lines above and below the box). In this particular example, we evaluated different targets for energy-related CO_2 emissions (x-axis) and different scenarios on technology availability (represented by different colors). Furthermore, we analyze the effect on the results of a particular example of the number of typical days and intraday clusters (Appendix A.2) and the length of the Sobol sequence (Appendix A.3).

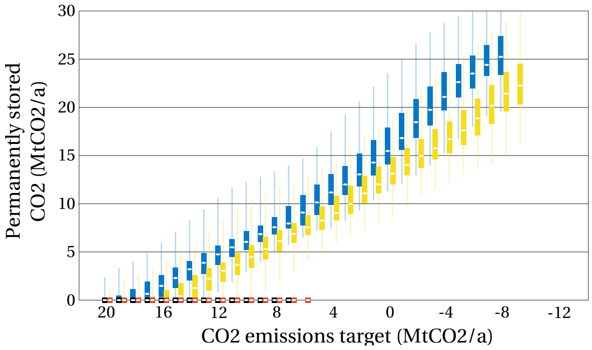

(a) Stored CO_2

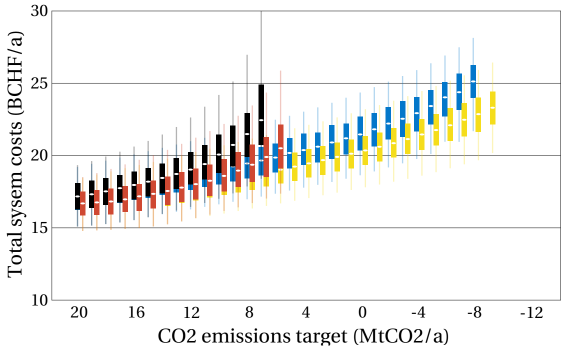

(b) Total system costs

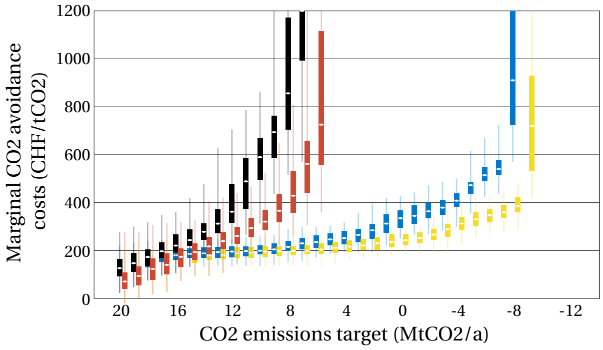

(c) Marginal CO_2 costs

Figure 5.2: Typical model results for selected variables at different CO_2 targets in four scenarios

Appendices

Appendix A

Model results

A.1 Effect of number of typical days and intra-day clusters

Figure A.1 shows the time series for electricity supply and consumption for 12, 24 and 36 days at full 24-hour resolution. The basic seasonality of PV generation in summer and higher hydro power generation + imports in winter is visible in all variants. Also the typical pattern of the storage level in the hydro reservoirs is well reproduced. The storage level for pumped hydro shows the expected daily variation which is comparable for the three typical day cases, the pattern repeats simply more often for 36 typical days. The small black dots mark the storage level at midnight which is forced to be identical for all days. Figures A.2a and A.2b show the same electricity time series for 12 and 24 typical days, respectively, now varying the clustering. Despite the crude approximation by three 8-hour clusters, the basic daily pattern is still visible.

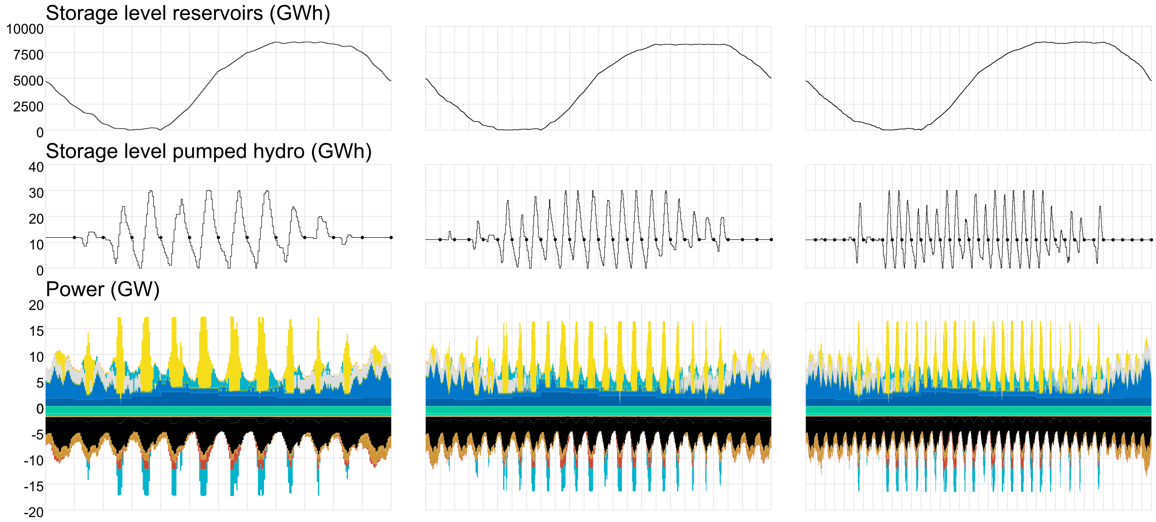

Figure A.1: Electricity supply and demand for 12 (left), 24 (mid) and 36 (right) typical days, full 24 hour resolution: photovoltaics pumped hydro storage thermal power hydro power mobility base demand heat pumps electric heaters

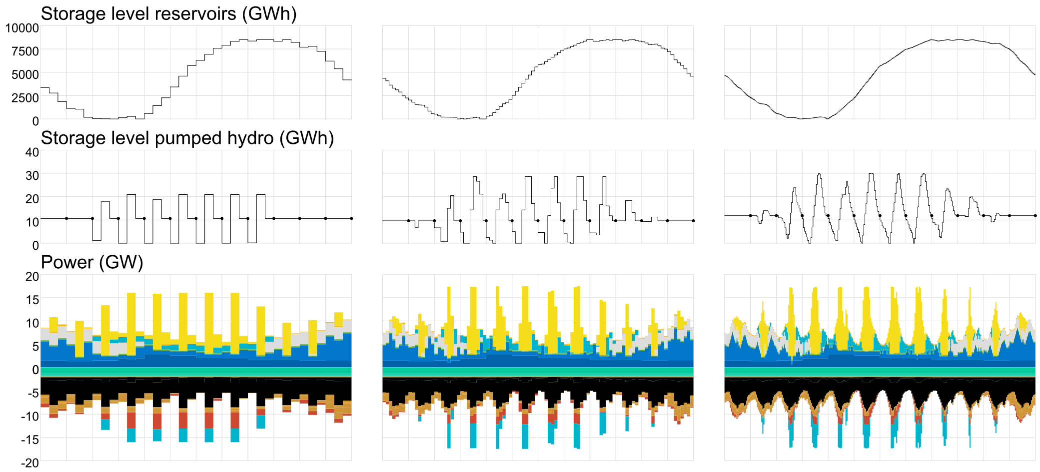

(a) 12 typical days

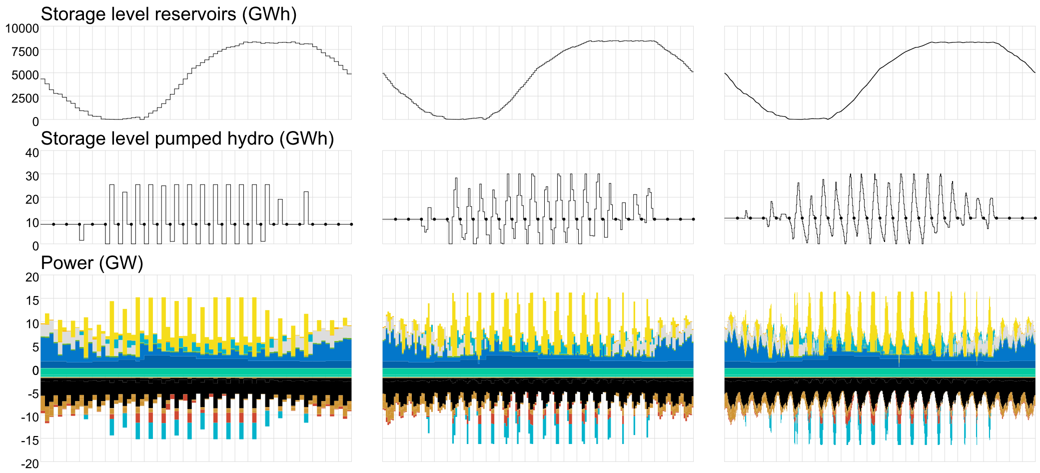

(b) 24 typical days

Figure A.2: Electricity supply and demand for different number of typical days and 3 (left), 8 (mid) and 24 (right) intra-day clusters: photovoltaics pumped hydro storage thermal power hydro power mobility base demand heat pumps electric heaters

A.2 Effect of the choice of typical days and intra-day clusters on the uncertainty analysis

We carried out a Monte Carlo analysis to evaluate the impact of the choice of the number of typical days and the intra-day clusters on the aforementioned statistical quantities. We simulate one scenario variant for a CO_2 target of 0, -5 and -10 $MtCO_2$/a for 12, 24 and 36 typical days and 3, 8 and 24 intra-day clusters. Figure A.3 shows the results for different model variables. Each group of results contains 9 box-plots, from left to right these are 3/8/24 intra-day clusters for 12 typical days, then 3/8/24 for 24 typical days and finally 3/8/24 for 36 typical days. The boxplot marked in black is a strategy with 8 intra-day clusters and 24 typical days.

For many variables, the basic statistical parameters such as median and inter-quartile range are rather stable towards the temporal resolution. We can see some differences for the lowest resolution of 12 typical days and 3 or 8 intra-day cluster for hydrogen production and industrial electrical heaters. We found the largest scatter for the storage output of pumped hydro and especially thermal storage. This is not surprising since the clustering of hours within a day is effectively a low pass filter that mimics a storage of several hours. Therefore, less *real* thermal storage is required for those cases. The general increase of total system costs with time resolution is also related to this fact: clustering reduces the peaks and leads therefore to an under-sizing of certain assets such as heat pumps.

The number of periods from the lowest to the highest resolution varies from 36 (12 typical days × 3 clusters) to 864 (36×24), which implies a factor of 24-fold. However, this factor translates into an even larger difference in computing time, since normally it scales higher than the number of unknowns. Therefore, we chose, as a practical compromise, the combination of 24 typical days and 8 clusters of 3 hours (the black boxplots).

A.3 Effect of Sobol sequence length

A further aspect that strongly influences the required computation time is the length of a Sobol sequence. It has to be chosen such that the fundamental statistical parameters such as the median, quartile ranges and minimum/maximum of any quantity can be properly evaluated. Figure A.4 shows the statistics for the same indicators as before, varying the Sobol sequence length from 10, 20, 50, 100, 200, 500 and 1000. We can see that the shortest sequences differ strongly from the longer ones. From a length of 100 (shown in black) the basic statistical parameters are stable. Therefore, we choose a sequence length of 100.

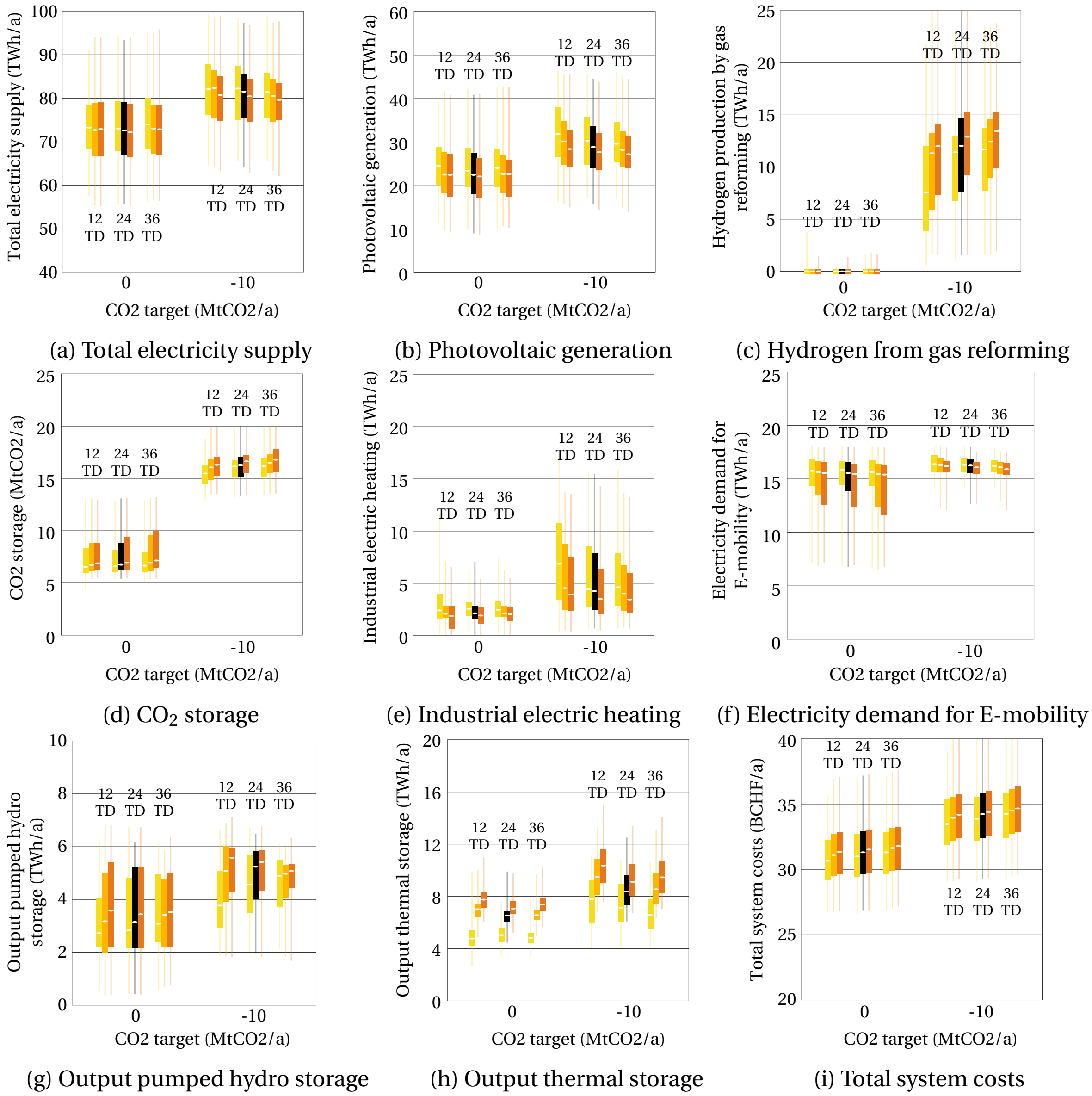

(a) Total electricity supply (b) Photovoltaic generation (c) Hydrogen from gas reforming

(d) CO_2 storage (e) Industrial electric heating (f) Electricity demand for E-mobility

(g) Output pumped hydro storage (h) Output thermal storage (i) Total system costs

Figure A.3: Selected model results for various combinations of typical days (TD) and intra-day clusters; from left to right: 12/03, 12/08, 12/24, 24/03, 24/08, 24/24, 36/03, 36/08, 36/24; 24/08 strategy marked in black

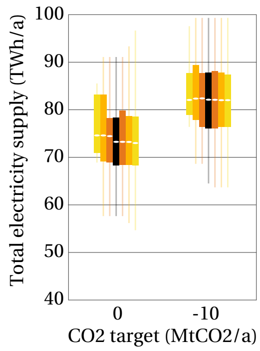

(a) Total electricity supply

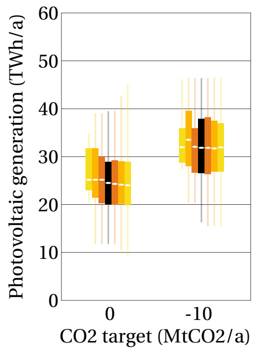

(b) Photovoltaic generation

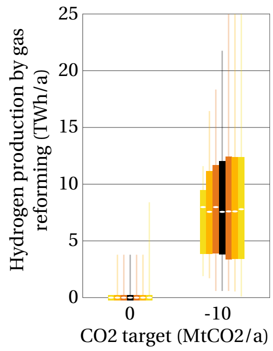

(c) Hydrogen from gas reforming

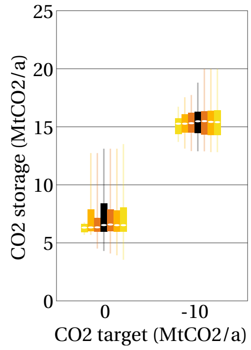

(d) CO_2 storage

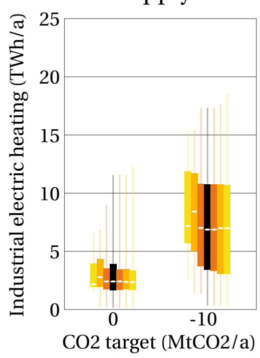

(e) Industrial electric heating

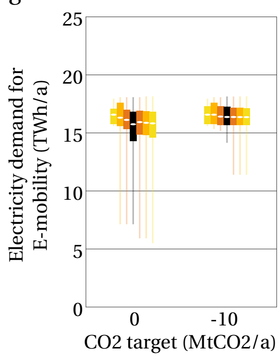

(f) Electricity demand for E-mobility

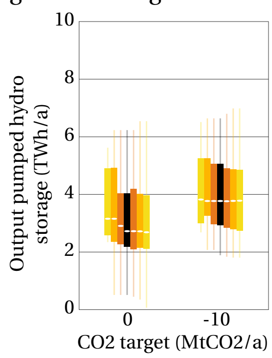

(g) Output pumped hydro storage

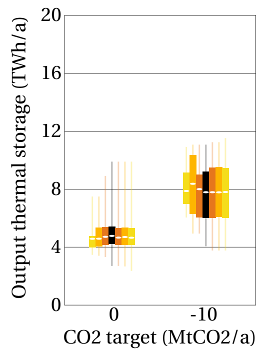

(h) Output thermal storage

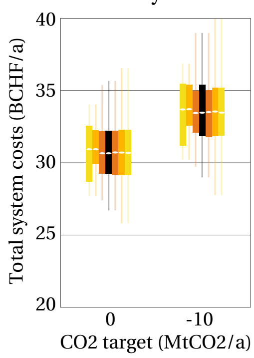

(i) Total system costs

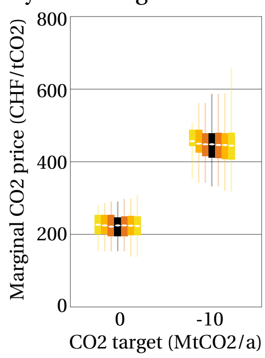

(j) Marginal CO_2 price

Figure A.4: Selected model results for various Sobol sequence length; from left to right: 10, 20, 50, 100, 200, 500 and 1000; length of 100 marked in black

Appendix B

Demands

This appendix presents the demands calculated using the drivers in Marcucci et al. (2020) (Table 3.2). The historical data is from the BFE (2018), Analysis of energy consumption 2000—2017 by specific use (*Analyse des schweizerischen Energieverbrauchs 2000–2017 nach Verwendungszwecken*), assuming the following sectoral efficiencies to convert from final to useful energy demand: (1) Space heating: 86% from Streicher et al. (2020b); (2) Warm water: 80%; and (3) Process heat: 70%.

B.1 Space Heating

B.1.1 Energy reference area

Table B.1: Projected Sectoral Energy Reference Area (Mm2)

Variant	**2010**	**2018**	**2020**	**2030**	**2040**	**2050**	**2060**	**2010–2060**
Residential (Mm2)								
Reference	443.7	494.6	507.6	562.2	602.3	630	652.7	0.77% p.a.
High	443.7	494.6	508	577.3	636.6	686	730.5	1% p.a.
Low	443.7	494.6	507.1	546.8	566.3	570.1	567.8	0.49% p.a.
Commercial (Mm2)								
Reference	194.3	216.5	219.4	240.5	256	266.7	275.4	0.7% p.a.
High	194.3	216.5	219.5	246.3	269.2	288.3	305.5	0.91% p.a.
Low	194.3	216.5	219.2	234.5	242.1	243.5	242.6	0.45% p.a.
Industry (Mm2)								
Reference	87.4	92.8	94.1	98.8	103.4	107.4	111	0.48% p.a.
High	87.4	92.8	94.2	100.4	106.1	111.2	115.9	0.57% p.a.
Low	87.4	92.8	93.9	97.4	100.8	103.6	105.7	0.38% p.a.

> Data available at https://data.sccer-jasm.ch/era/

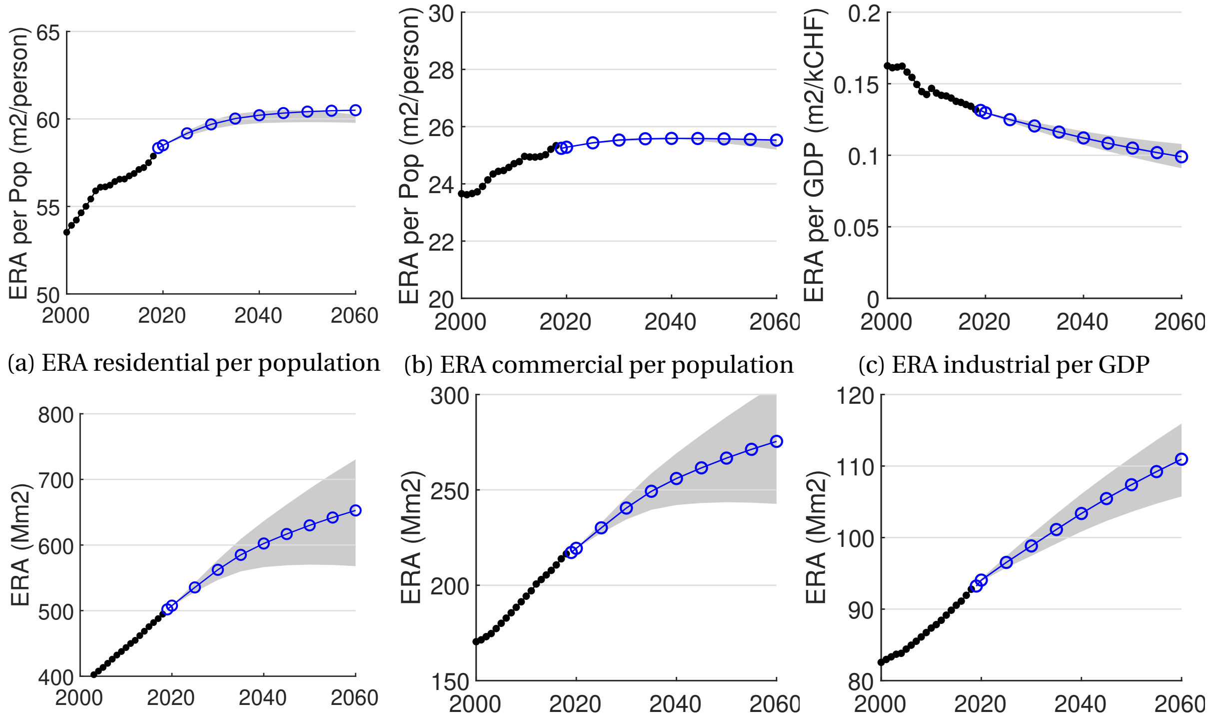

(a) ERA residential per population (b) ERA commercial per population (c) ERA industrial per GDP

(d) ERA residential (Mm^2) (e) ERA commercial (Mm^2) (f) ERA industrial (Mm^2)

Figure B.1: Sectoral Energy reference area

Table B.2: Residential Energy Reference Area by age (Mm2)

Age	2016	2020	2030	2040	2050	2060	2020–2060
Single family houses							
<1920	42	41.4	39.6	37.3	34.6	31.5	-0.69% p.a.
1920-1945	22.2	21.8	20.6	19	17	14.6	-0.98% p.a.
1946-1960	21	20.6	19.9	18.8	17.3	15.3	-0.74% p.a.
1961-1970	18.9	18.7	18.2	17.3	16.2	14.6	-0.62% p.a.
1971-1980	25	24.9	24.3	23.5	22.2	20.3	-0.51% p.a.
1981-1990	27.7	27.6	27.2	26.5	25.4	23.6	-0.39% p.a.
1991-2000	24.5	24.5	24.2	23.7	22.7	21.1	-0.37% p.a.
2001-2010	23.8	23.7	23.5	23.1	22.1	20.7	-0.34% p.a.
2011-2017	10.8	13.6	13.6	13.4	13.1	12.4	-0.23% p.a.
>2017							
Reference	0	5.6	20.8	33.3	44.4	57.7	5.99% p.a.
High	0	5.8	24.6	41.9	58.4	77.1	6.71% p.a.
Low	0	5.5	16.9	24.3	29.4	36.5	4.83% p.a.
Multi family houses							
<1920	37.5	37.7	37.5	37.2	36.6	35.4	-0.16% p.a.
1920-1945	21.8	21.8	21.7	21.6	21.4	20.9	-0.1% p.a.

Table B.2: Residential Energy Reference Area by age (Mm2) (continued)

Age	**2016**	**2020**	**2030**	**2040**	**2050**	**2060**	**2020–2060**
1946-1960	28	27.9	27.8	27.3	25.5	20.8	-0.73% p.a.
1961-1970	37.6	37.8	37.8	37.5	36.3	32.2	-0.4% p.a.
1971-1980	33.8	34.1	34.1	34	33.5	31.4	-0.21% p.a.
1981-1990	27.3	27.6	27.6	27.6	27.4	26.5	-0.1% p.a.
1991-2000	25.5	25.7	25.7	25.7	25.6	25.2	-0.05% p.a.
2001-2010	30.2	30.3	30.3	30.3	30.3	30.2	-0.01% p.a.
2011-2017	24.4	25.3	25.3	25.3	25.3	25.3	0% p.a.
>2017							
Reference	0	16.9	62.4	99.9	133.2	173	5.99% p.a.
High	0	17.3	73.7	125.6	175.2	231.3	6.71% p.a.
Low	0	16.6	50.8	72.9	88.3	109.4	4.83% p.a.

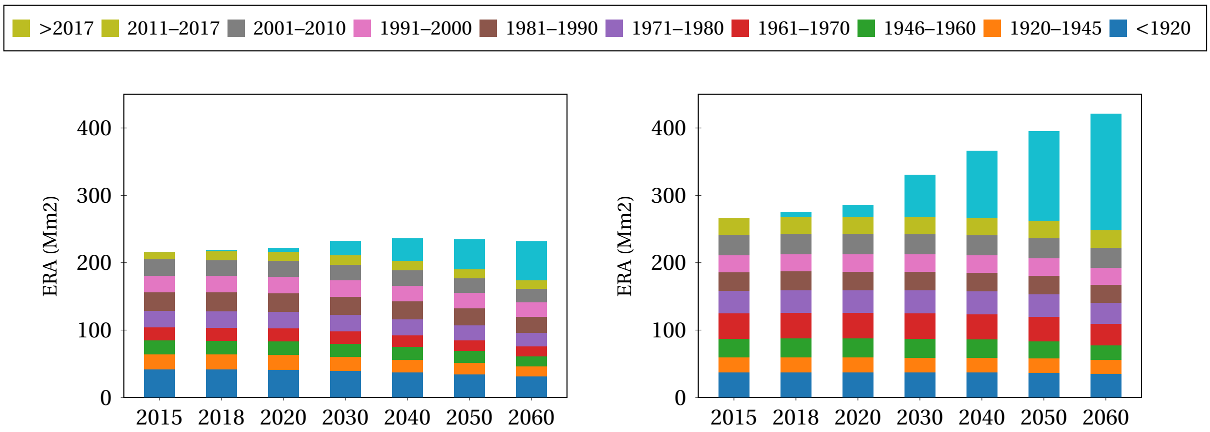

(a) Single family houses

(b) Multi family houses

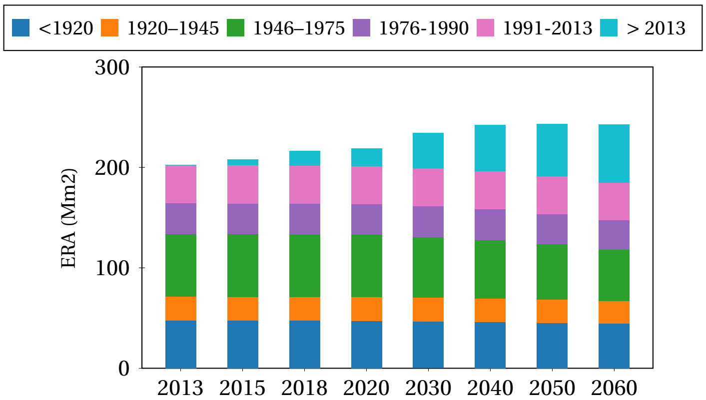

(c) Commercial buildings (including temporarily used houses)

Figure B.2: ERA by age in the residential and commercial sectors for the reference scenario

B.1.2 Space heating demand

Table B.3: Projected space heating demand (Useful energy in TWh)

Variant	Climate	2010[a]	2018	2020	2030	2040	2050	2060	2010–2060
Residential (TWh)									
Reference	Constant	46	34.7	37.3	38.7	39.2	38.8	37.2	-0.42% p.a.
	RCP 2.6	46	34.7	38.7	39.5	39.4	38.6	36.8	-0.45% p.a.
	RCP 4.5	46	34.7	39.2	39.6	38.9	37.5	35.1	-0.54% p.a.
	RCP 8.5	46	34.7	38.5	38.8	37.9	35.7	32.8	-0.67% p.a.
High	Constant	46	34.7	37.4	39.2	40.2	40.3	39.1	-0.32% p.a.
Low	Constant	46	34.7	37.3	38.2	38.2	37.2	35.2	-0.53% p.a.
Commercial (TWh)									
Reference	Constant	18.6	14.1	15.5	16.1	16.4	16.4	16.2	-0.27% p.a.
	RCP 2.6	18.6	14.1	16	16.4	16.5	16.4	16.1	-0.29% p.a.
	RCP 4.5	18.6	14.1	16.2	16.5	16.3	15.9	15.3	-0.39% p.a.
	RCP 8.5	18.6	14.1	15.9	16.1	15.9	15.1	14.3	-0.52% p.a.
High	Constant	18.6	14.1	15.5	16.3	16.9	17.1	17.1	-0.17% p.a.
Low	Constant	18.6	14.1	15.4	15.9	16	15.7	15.3	-0.39% p.a.
Industrial (TWh)									
Reference	Constant	5.5	3.5	3.5	3.3	3.2	3	2.9	-1.29% p.a.
	RCP 2.6	5.5	3.5	3.6	3.4	3.2	3	2.9	-1.31% p.a.
	RCP 4.5	5.5	3.5	3.7	3.4	3.1	2.9	2.7	-1.4% p.a.
	RCP 8.5	5.5	3.5	3.6	3.3	3.1	2.8	2.5	-1.53% p.a.
High	Constant	5.5	3.5	3.5	3.4	3.3	3.1	3	-1.2% p.a.
Low	Constant	5.5	3.5	3.5	3.3	3.1	2.9	2.7	-1.38% p.a.

[a] We calculate useful energy demand from the final energy statistics (BFE, 2018), assuming an efficiency of 86%.

Data available at https://data.sccer-jasm.ch/end-use-energy-demand-ses/

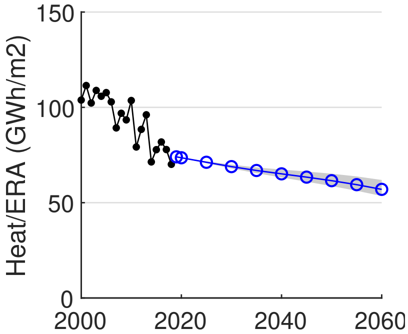

(a) Residential demand per ERA

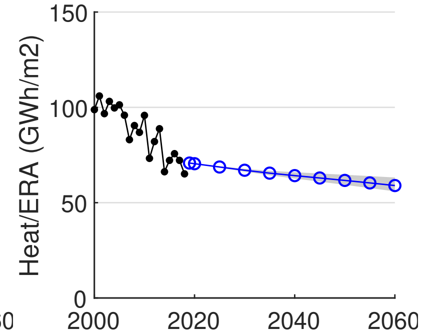

(b) Commercial demand per ERA

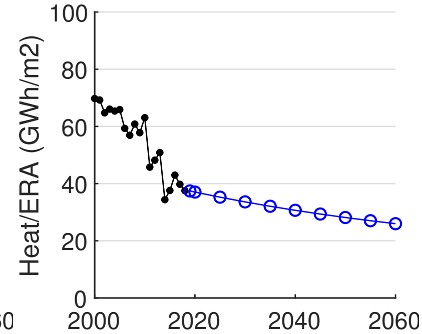

(c) Industrial demand per ERA

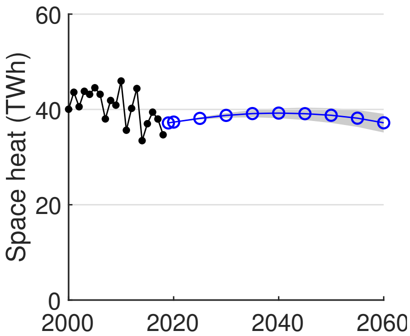

(d) Residential total demand

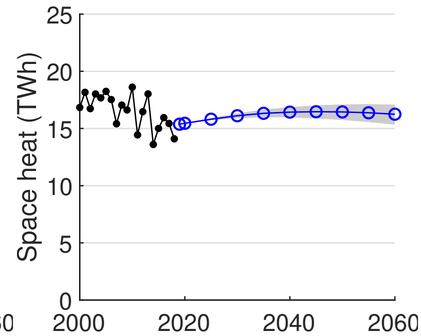

(e) Commercial total demand

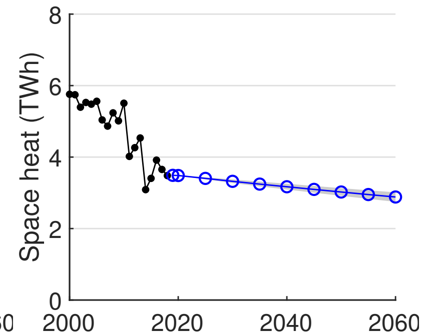

(f) Industrial total demand

Figure B.3: Space heating demand for constant climate

B.2 Warm water

Table B.4: Warm water demand (Useful energy in TWh)

Variant	2010[a]	2018	2020	2030	2040	2050	2060	2010–2060
Residential (TWh)								
Reference	7.2	7.1	7.1	7.4	7.6	7.7	7.9	0.2% p.a.
High	7.2	7.1	7.1	7.6	8	8.4	8.9	0.44% p.a.
Low	7.2	7.1	7.1	7.2	7.2	7.1	7	-0.05% p.a.
Commercial (TWh)								
Reference	2.36	2.44	2.46	2.57	2.65	2.71	2.77	0.32% p.a.
High	2.36	2.44	2.46	2.63	2.79	2.94	3.12	0.55% p.a.
Low	2.36	2.44	2.46	2.51	2.51	2.47	2.44	0.06% p.a.
Industrial (TWh)								
Reference	0.86	0.55	0.55	0.56	0.59	0.62	0.66	-0.53% p.a.
High	0.86	0.55	0.55	0.59	0.63	0.68	0.75	-0.27% p.a.
Low	0.86	0.55	0.55	0.54	0.55	0.56	0.58	-0.8% p.a.

[a]We calculate useful energy demand from the final energy statistics (BFE, 2018), assuming an efficiency of 80%.

Data available at https://data.sccer-jasm.ch/end-use-energy-demand-ses/

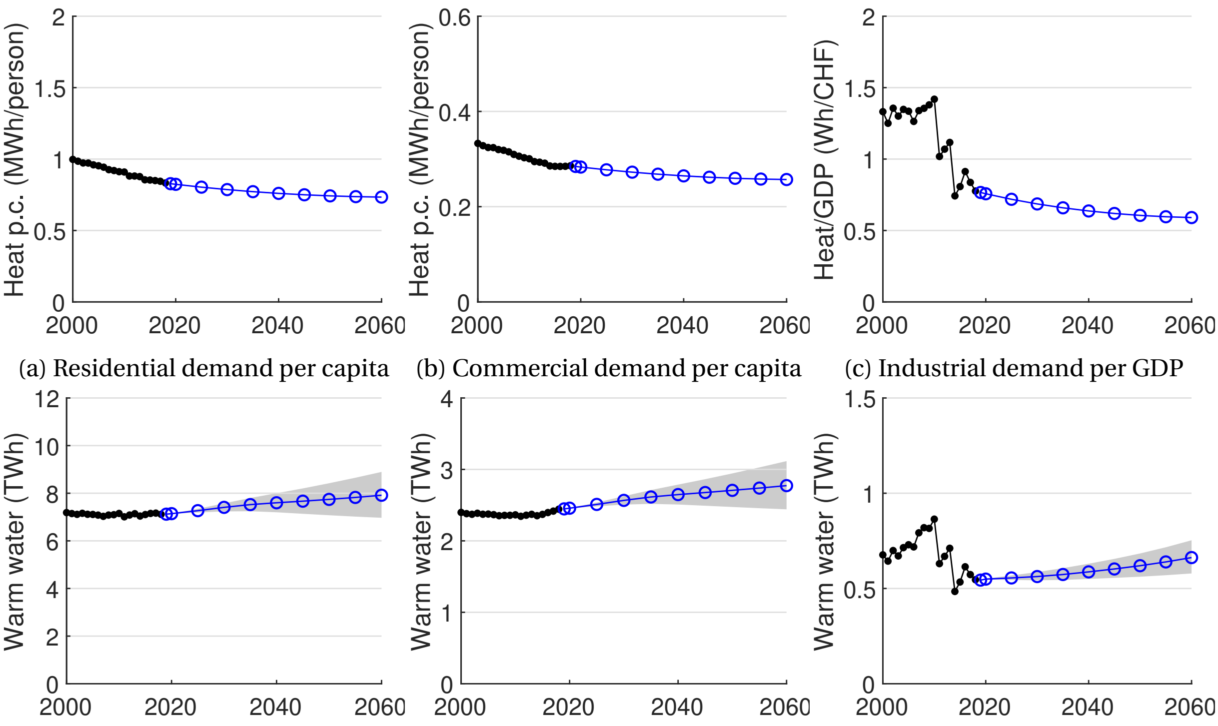

(a) Residential demand per capita (b) Commercial demand per capita (c) Industrial demand per GDP

(d) Residential total demand (e) Commercial total demand (f) Industrial total demand

Figure B.4: Warm water demand (useful energy)

B.3 Process heat

Table B.5: Process heat demand (Useful energy in TWh)

Variant	**2010**[a]	**2018**	**2020**	**2030**	**2040**	**2050**	**2060**	**2010–2060**
Commercial (TWh)								
Reference	0.5	0.42	0.42	0.37	0.34	0.31	0.3	-1.04% p.a.
High	0.5	0.42	0.42	0.39	0.36	0.35	0.34	-0.78% p.a.
Low	0.5	0.42	0.41	0.36	0.32	0.28	0.26	-1.3% p.a.
Industrial (TWh)[b]								
Reference	19.2	18.7	18.8	18.9	19.3	19.6	20	0.08% p.a.
High	19.2	18.7	18.9	19.7	20.7	21.6	22.8	0.34% p.a.
Low	19.2	18.7	18.7	18.3	18.1	17.8	17.5	-0.19% p.a.

[a]We calculate useful energy demand from the final energy statistics (BFE, 2018), assuming an efficiency of 70%.

[b]Industrial process heat corresponds to the categories *Prozesswärme* and *sonstige* in BFE (2018, Table 28)

Data available at https://data.sccer-jasm.ch/end-use-energy-demand-ses/

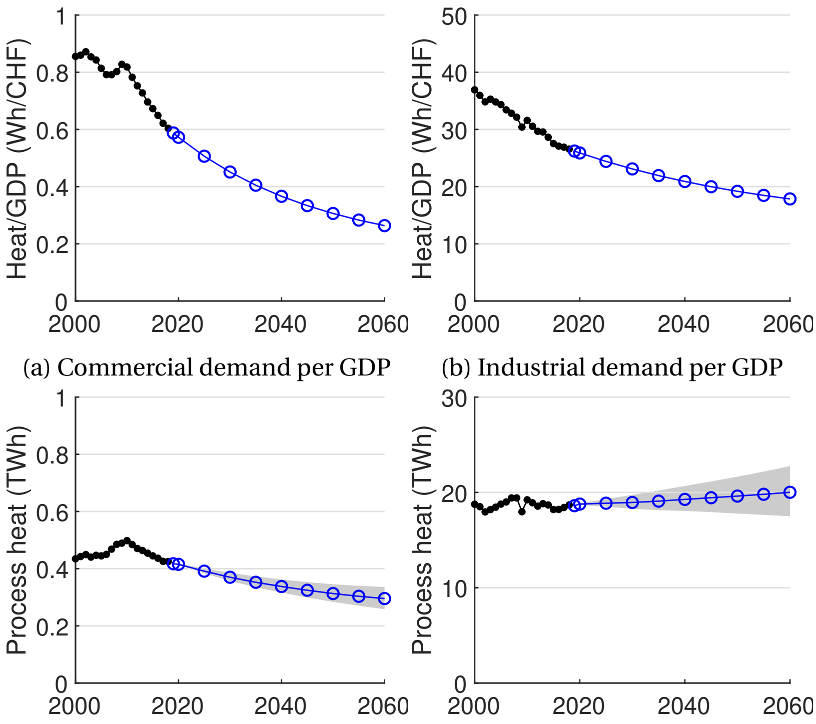

(a) Commercial demand per GDP (b) Industrial demand per GDP

(c) Commercial total demand (d) Industrial total demand

Figure B.5: Total process heat demand (useful energy)

B.4 Electricity: Electric appliances

Table B.6: Electricity demand (Useful energy in TWh)

Variant	2010	2018	2020	2030	2040	2050	2060	2010–2060
Residential (TWh)								
Reference	12.7	12.4	12.4	12.5	12.3	12	11.7	-0.17% p.a.
High	12.7	12.4	12.4	12.8	13	13.1	13.1	0.06% p.a.
Low	12.7	12.4	12.4	12.2	11.7	11	10.3	-0.43% p.a.
Commercial (TWh)								
Reference	15.5	15.1	15.1	14.9	14.5	14	13.4	-0.3% p.a.
High	15.5	15.1	15.2	15.5	15.6	15.5	15.2	-0.04% p.a.
Low	15.5	15.1	15	14.3	13.6	12.7	11.7	-0.56% p.a.
Industrial (TWh)								
Reference	12.9	11.5	11.5	11.4	11.6	12.2	13.1	0.03% p.a.
High	12.9	11.5	11.5	11.8	12.5	13.4	14.9	0.29% p.a.
Low	12.9	11.5	11.4	11	10.9	11	11.4	-0.23% p.a.

Data available at https://data.sccer-jasm.ch/end-use-energy-demand-ses/

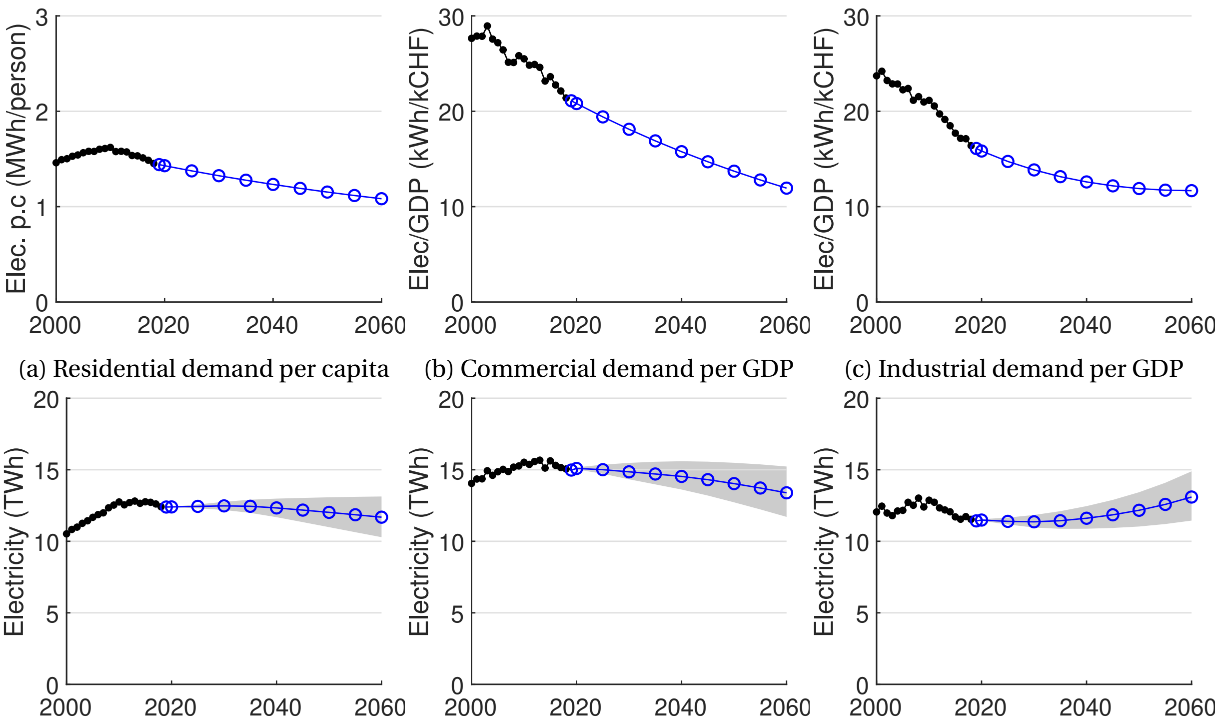

(a) Residential demand per capita (b) Commercial demand per GDP (c) Industrial demand per GDP

(d) Residential total demand (e) Commercial total demand (f) Industrial total demand

Figure B.6: Electricity demand

B.5 Transport

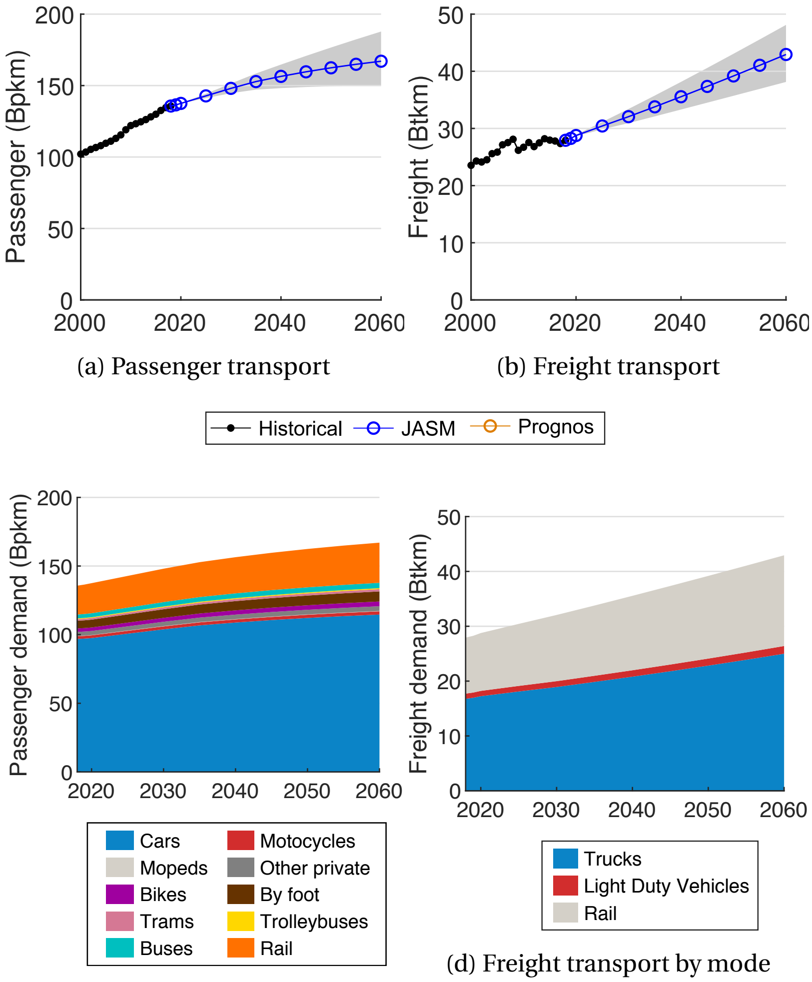

(a) Passenger transport

(b) Freight transport

(c) Passenger demand by mode

(d) Freight transport by mode

Figure B.7: Transport demand

Table B.7: Passenger transport demand (Billion pkm) based on ARE (2016)

Mode	2010	2020	2030	2040	2050[a]	2060[a]	2010-2060
Reference							
Personal cars	85.93	97.5	103.87	108.83	112.17	114.63	0.58% p.a.
Motorcycles	2.3	2.04	2.17	2.27	2.34	2.39	0.08% p.a.
Mopeds and fast e-bikes	0.13	0.18	0.19	0.2	0.21	0.21	0.94% p.a.
Other private	2.5	2.95	3.15	3.3	3.4	3.47	0.66% p.a.
Bikes	2.12	2.56	2.85	3.1	3.29	3.45	0.98% p.a.
On foot	5.47	5.69	6.29	6.75	7.09	7.35	0.59% p.a.
Trams	0.98	1.22	1.36	1.47	1.56	1.63	1.03% p.a.
Trolleybuses	0.52	0.55	0.61	0.67	0.71	0.74	0.72% p.a.
Buses	2.49	2.91	3.23	3.5	3.71	3.89	0.89% p.a.
Passenger rail	19.59	21.9	24.32	26.34	27.95	29.25	0.81% p.a.
High							
Personal cars	85.93	97.57	106.24	114.58	121.97	128.86	0.81% p.a.
Motorcycles	2.3	2.04	2.22	2.39	2.55	2.69	0.32% p.a.
Mopeds and fast e-bikes	0.13	0.18	0.2	0.21	0.22	0.24	1.17% p.a.
Other private	2.5	2.96	3.22	3.47	3.7	3.91	0.9% p.a.
Bikes	2.12	2.56	2.92	3.26	3.58	3.89	1.22% p.a.
On foot	5.47	5.7	6.44	7.11	7.71	8.25	0.83% p.a.
Trams	0.98	1.22	1.39	1.55	1.7	1.84	1.27% p.a.
Trolleybuses	0.52	0.55	0.63	0.7	0.77	0.83	0.96% p.a.
Buses	2.49	2.91	3.3	3.68	4.04	4.38	1.13% p.a.
Passenger rail	19.59	21.92	24.88	27.74	30.41	32.94	1.04% p.a.
Low							
Personal cars	85.93	97.44	101.48	103.12	103.41	103.51	0.37% p.a.
Motorcycles	2.3	2.03	2.12	2.15	2.16	2.16	-0.12% p.a.
Mopeds and fast e-bikes	0.13	0.18	0.19	0.19	0.19	0.19	0.73% p.a.
Other private	2.5	2.95	3.08	3.12	3.13	3.14	0.46% p.a.
Bikes	2.12	2.55	2.79	2.93	3.02	3.07	0.75% p.a.
On foot	5.47	5.69	6.15	6.4	6.52	6.58	0.37% p.a.
Trams	0.98	1.22	1.33	1.39	1.43	1.46	0.8% p.a.
Trolleybuses	0.52	0.55	0.6	0.63	0.65	0.66	0.49% p.a.
Buses	2.49	2.91	3.16	3.32	3.41	3.46	0.66% p.a.
Passenger rail	19.59	21.89	23.77	24.96	25.64	26.05	0.57% p.a.

[a] ARE projections go to 2040, we assume a trend that follows our population and GDP projections.

Data available at https://data.sccer-jasm.ch/end-use-energy-demand-ses/

Table B.8: Freight transport demand (Billion tkm) based on ARE (2016)

Scenario	2010	2020	2030	2040	2050[a]	2060[a]	2010-2060
Reference							
Trucks	16.01	17.24	18.92	20.81	22.82	24.99	0.89% p.a.
Light Duty Vehicles	0.9	0.97	1.07	1.17	1.28	1.41	0.9% p.a.
Freight rail	9.81	10.55	12.08	13.57	15.08	16.54	1.05% p.a.
High							
Trucks	16.01	17.33	19.71	22.32	25.07	27.98	1.12% p.a.
Light Duty Vehicles	0.9	0.98	1.11	1.26	1.41	1.58	1.13% p.a.
Freight rail	9.81	10.6	12.58	14.56	16.58	18.56	1.28% p.a.
Low							
Trucks	16.01	17.17	18.25	19.49	20.8	22.2	0.66% p.a.
Light Duty Vehicles	0.9	0.97	1.03	1.1	1.17	1.25	0.66% p.a.
Freight rail	9.81	10.5	11.65	12.72	13.74	14.68	0.81% p.a.

[a] ARE projections go to 2040, we assume a trend that follows our population and GDP projections.

Data available at https://data.sccer-jasm.ch/end-use-energy-demand-ses/

B.6 Summary

Summarizing the results of the previous sections, Figure B.8 shows the total demand for electricity, space heat, warm water and process heat, summed up over the three sectors.

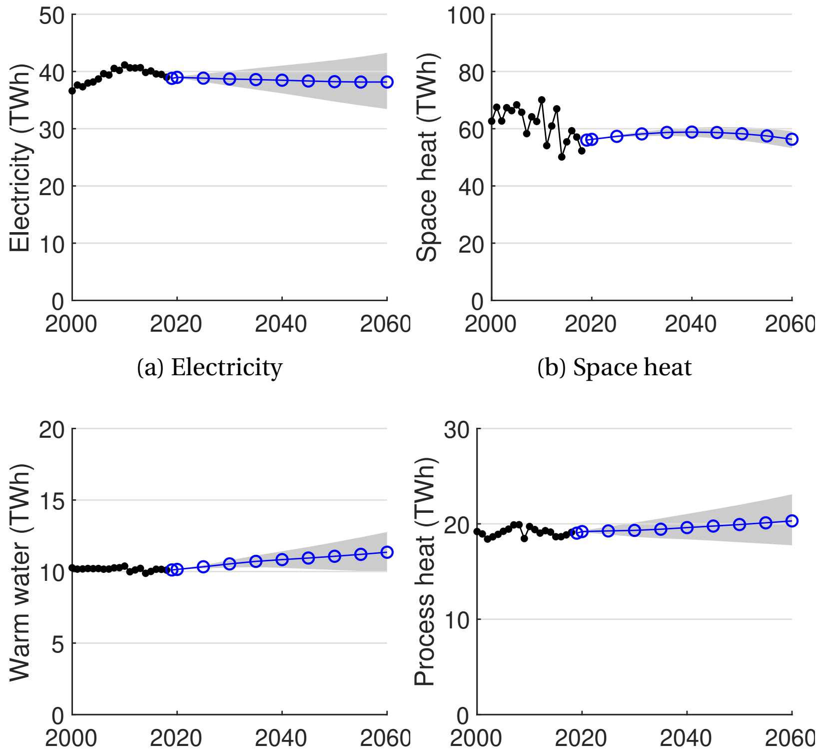

(a) Electricity (b) Space heat

(c) Warm water (d) Process heat

Figure B.8: Total energy demand

Bibliography

ARE, 2016. Perspektiven des Schweizerischen Personen- und Güterverkehrs bis 2040. Technical Report. Bundesamt fr̈ Raumentwicklung (ARE).

ARE, 2017. Sachpläne und Konzepte - Konzept Windenergie. Basis zur Berücksichtigung der Bundesinteressen bei der Planung von Windenergieanlagen.

Assouline, D., Mohajeri, N., Scartezzini, J.L., 2017. Quantifying rooftop photovoltaic solar energy potential: A machine learning approach. Solar Energy 141, 278–296. URL: http://www.sciencedirect.com/science/article/pii/S0038092X16305850, doi:https://doi.org/10.1016/j.solener.2016.11.045.

Assouline, D., Mohajeri, N., Scartezzini, J.L., 2018. Large-scale rooftop solar photovoltaic technical potential estimation using random forests. Applied Energy 217, 189–211. URL: http://www.sciencedirect.com/science/article/pii/S0306261918302496, doi:https://doi.org/10.1016/j.apenergy.2018.02.118.

Bauer, C., Cox, B., Heck, T., Zhang, X., 2019. Potentials, costs and environmental assessment of electricity generation technologies – An update of electricity generation costs and potentials. Technical Report. Paul Scherrer Institut. URL: https://www.bfe.admin.ch/bfe/de/home/news-und-medien/publikationen/_jcr_content/par/externalcontent.external.exturl.pdf/aHR0cHM6Ly9wdWJkYi5iZmUuYWRtaW4uY2gvZGUvcHVibGljYX/Rpb24vZG93bmxvYWQvOTgyNi5wZGY=.pdf.

Bauer, C., Hirschberg, S., Bäuerle, Y., Biollaz, S., Calbry-Muzyka, A., Cox, B., Heck, T., Lehnert, M., Meier, A., Prasser, H.M., Schenler, W., Treyer, K., Vogel, F., Wieckert, H., Zhang, X., Zimmermann, M., Burg, V., Bowman, G., Erni, M., Saar, M., Tran, M., 2017. Potentials, costs and environmental assessment of electricity generation technologies. Technical Report. Paul Scherrer Institut.

Berger, M., Worlitschek, J., 2019. The link between climate and thermal energy demand on national level: A case study on switzerland. Energy and Buildings 202, 109372. URL: http://www.sciencedirect.com/science/article/pii/S037877881931120X, doi:https://doi.org/10.1016/j.enbuild.2019.109372.

BFE, 2017a. Schweizerische Elektrizitätsstatistik 1998–2017. Technical Report. Bundesamt für Energie. URL: https://www.bfe.admin.ch/bfe/en/home/supply/statistics-and-geodata/energy-statistics/electricity-statistics.html.

BFE, 2017b. Schweizerische Statistik der erneuerbaren Energien. URL: https://www.bfe.admin.ch/bfe/de/home/versorgung/statistik-und-geodaten/energiestatistiken/teilstatistiken.html.

BFE, 2018. Analysis of energy consumption 2000–2017 by specific use (Analyse des schweizerischen Energieverbrauchs 2000 – 2017 nach Verwendungszwecken). Technical Report. BFE. URL: https://www.bfe.admin.ch/bfe/en/home/supply/statistics-and-geodata/energy-statistics/analysis-of-energy-consumption-by-specific-use.html.

BFE, 2019a. Elektrizitätsproduktion der Schweiz - Wasserkraft nach Kraftwerkstyp. Technical Report. Bundesamt für Energie. URL: https://www.bfe.admin.ch/bfe/en/home/supply/statistics-and-geodata/energy-statistics/electricity-statistics.html.

BFE, 2019b. Gesamte Erzeugung und Abgabe elektrischer Energie in der Schweiz 1999–201. URL: https://www.bfe.admin.ch/bfe/de/home/news-und-medien/open-government-data.exturl.html/aHR0cHM6Ly9wdWJkYi5iZmUuYWRtaW4uY2gvZGUvc3VjaGU_a2/V5d29yZHM9Mzkw.html.

BFE, 2019c. Schweizer hausdächer und -fassaden könnten jährlich 67 Twh Solarstrom produzieren. URL: https://www.bfe.admin.ch/bfe/de/home/news-und-medien/medienmitteilungen/mm-test.msg-id-74641.html.

BFS, 2019a. Transportleistungen im Güterverkehr, je-d-11.05.01.02. URL: https://www.bfs.admin.ch/bfs/de/home/statistiken/mobilitaet-verkehr/gueterverkehr.assetdetail.10607212.html.

BFS, 2019b. Verkehrsleistungen im Personenverkehr, je-d-11.04.01.02. URL: https://www.bfs.admin.ch/bfs/de/home/statistiken/mobilitaet-verkehr/personenverkehr/leistungen.assetdetail.11207451.html.

BFS, 2019c. Öffentlicher Verkehr (inkl. Schienengüterverkehr) – detaillierte Zeitreihen, su-d-11-tp-zr. URL: https://www.bfs.admin.ch/bfs/en/home/news/whats-new.assetdetail.11207458.html.

BFS, 2020. Szenarien zur Bevölkerungsentwicklung der Schweiz und der Kantone 2020-2050. Technical Report. Bundesamt für Statistik. https://www.bfs.admin.ch/asset/de/px-x-0104000000_102 and https://www.bfs.admin.ch/bfs/de/home/statistiken/kataloge-datenbanken.gnpdetail.2020-0194.html.

Brown, A., Waldheim, L., Landälv, I., Saddler, J., Ebadian, M., McMillan, J.D., Bonomi, A., Klein, B., 2020. Advanced Biofuels - Potential for Cost Reduction. Technical Report. IEA Bioenergy.

Buffat, R., Grassi, S., Rauball, M., 2018. A scalable method for estimating rooftop solar irradiation potential over large regions. Applied Energy 216, 389–401. URL: https://doi.org/10.1016/j.apenergy.2018.02.008.

Cattin, R., Schaffner, B., Humar-Maegli, T., Albrecht, S., Re-mund, J., Klauser, D., Engel, J.J., 2012. Berechnung der Energiepotenziale für Wind- und Sonnenenergie. Technical Report. Meteotest - commissioned by Bundesamtes für Umwelt (BAFU).

CH2018, 2018. CH2018 – Climate Scenarios for Switzerland. Technical Report. National Centre for Climate Services.

Christensen, A., 2020. Assessment of Hydrogen Production Costs from Electrolysis: United States and Europe. Technical Report. International Council on Clean Transportation. URL: https://theicct.org/sites/default/files/publications/final_icct2020_assessment_of%20_hydrogen_production_costs%20v2.pdf.

FAO, 2019. OECD-FAO Agricultural Outlook. Technical Report. FAO. doi:https://doi.org/10.1787/19991142.

Guidati, G., Marcucci, A., Damartzis, T., Burg, V., Schildhauer, T., Giardini, D., Kröcher, O., 2020. Biomass and waste potentials and conversion pathways for energy use in Switzerland. Technical Report. JASM and WSL. URL: https://sccer-jasm.ch/JASMpapers/JASM_biomass.pdf.

IEA, 2002. Potential for Building Integrated Photovoltaics. Technical Report. IEA.

IEA, 2017. Energy Technology Perspectives 2017. Technical Report. IEA. URL: https://www.iea.org/reports/energy-technology-perspectives-2017.

IEA, 2019. The Future of Hydrogen - Seizing today's opportunities. Technical Report. IEA. URL: https://www.iea.org/reports/the-future-of-hydrogen.

Iturralde, J., Alonso, L., Carrera, A., Salom, J., Battaglia, M., Carbonell, D., 2019. Energy demands for multi-family buildings in different climatic zones D1.1. URL: https://doi.org/10.5281/zenodo.3763249, doi:10.5281/zenodo.3763249.

Jakob, M., Catenazzi, G., Forster, R., Egli, T., Kaiser, T., Looser, R., Melliger, M., Nägeli, C., Reiter, U., Soini, M., Sunarjo, B., 2016. Erweiterung des Gebäudeparkmodells gemäss SIA-Effizienzpfad Energie. Technical Report. TEP Energy for the BFE. URL: http://www.tep-energy.ch/docs/2016_GEPAMOD_GPM_SIA_Effizienzpfad_Schlussbericht.pdf.

Jakob, M., Catenazzi, G., Forster, R., Egli, T., Lemon, T.K., Looser, R., Melliger, M., Nägeli, C., Reiter, U., Soini, M., Sunarjo, B., 2019. Erweiterung des Gebäudeparkmodells gemäss SIA-Effizienzpfad Energie. Technical Report. TEP Energy – Bundesamt für Energie (BFE). URL: https://www.tep-energy.ch/docs/2016_GEPAMOD_GPM_SIA_Effizienzpfad_Schlussbericht.pdf.

Keppo, I., Savola, T., 2007. Economic appraisal of small biofuel fired chp plants. Energy Conversion and Management 48, 1212 – 1221. URL: http://www.sciencedirect.com/science/article/pii/S0196890406003232, doi:https://doi.org/10.1016/j.enconman.2006.10.010.

Klauser, D., 2016. Solarpotentialanalyse für sonnendach.ch. URL: http://www.sciencedirect.com/science/article/pii/S0306261918302496.

Marcucci, A., Panos, E., Guidati, G., Lordan-Perret, R., Schlecht, I., Giardini, D., 2020. JASM framework and drivers definition. Technical Report. ETH Zurich, Paul Scherrer Institute and U. Basel - JASM. URL: https://sccer-jasm.ch/JASMpapers/JASM_drivers_framework.pdf.

Moret, S., 2017. Strategic energy planning under uncertainty. Ph.D. thesis. EPFL. URL: http://infoscience.epfl.ch/record/231814, doi:10.5075/epfl-thesis-7961.

Müller, D.B., 2006. Stock dynamics for forecasting material flows—case study for housing in the netherlands. Ecological Economics 59, 142 – 156. URL: http://www.sciencedirect.com/science/article/pii/S092180090500460X, doi:https://doi.org/10.1016/j.ecolecon.2005.09.025.

National Renewable Energy Laboratory, . Pvwatts® calculator. URL: https://pvwatts.nrel.gov/pvwatts.php.

Niederreiter, H., 1992. Random Number Generation and Quasi-Monte Carlo Methods. Society for Industrial and Applied Mathematics. URL: https://epubs.siam.org/doi/abs/10.1137/1.9781611970081, doi:10.1137/1.9781611970081, arXiv:https://epubs.siam.org/doi/pdf/10.1137/1.9781611970081.

NREL, 2011. Hydrogen Production Cost Estimate Using Biomass Gasification. Technical Report. National Renewable Energy Laboratory. URL: https://www.hydrogen.energy.gov/pdfs/51726.pdf.

OECD, 2001. Measuring capital. measurement of capital stocks, consumption of fixed capital and capital services.

Prognos, 2012. Die Energieperspektiven für die Schweiz bis 2050. URL: https://www.prognos.com/publikationen/alle-publikationen/292/show/7f9a4382d75cc40032147306d423aaca/.

Radov, D., Klevnäs, P., Hanif, A., Abu-Ebid, M., Barker, N., Stambaugh, J., 2009. The UK Supply Curve for Renewable Heat - Study for the Department of Energy and Climate Change. Technical Report. NERA economic consulting. URL: https://www.nera.com/content/dam/nera/publications/archive1/PUB_Renewable_Heat_July2009.pdf.

Ro, K.S., Cantrell, K., Elliott, D., Hunt, P.G., 2007. Catalytic Wet Gasification of Municipal and Animal Wastes. Industrial & Engineering Chemistry Research 46, 8839–8845. URL: https://pubs.acs.org/doi/10.1021/ie061403w, doi:10.1021/ie061403w.

Sandberg, N.H., Sartori, I., Heidrich, O., Dawson, R., Dascalaki, E., Dimitriou, S., Vimm-r, T., Filippidou, F., Stegnar, G., Šijanec Zavrl, M., Brattebø, H., 2016. Dynamic building stock modelling: Application to 11 european countries to support the energy efficiency and retrofit ambitions of the eu. Energy and Buildings 132, 26 – 38. URL: http://www.sciencedirect.com/science/article/pii/S0378778816304893, doi:https://doi.org/10.1016/j.enbuild.2016.05.100. towards an energy efficient European housing stock: monitoring, mapping and modelling retrofitting processes.

Sartori, I., Sandberg, N.H., Brattebø, H., 2016. Dynamic building stock modelling: General algorithm and exemplification for norway. Energy and Buildings 132, 13 – 25. URL: http://www.sciencedirect.com/science/article/pii/S037877881630487X, doi:https://doi.org/10.1016/j.enbuild.2016.05.098. towards an energy efficient European housing stock: monitoring, mapping and modelling retrofitting processes.

Savelsberg, J., Schillinger, M., Schlecht, I., Weigt, H., 2018. The impact of climate change on swiss hydro power. Sustainability 10, 2541. URL: https://doi.org/10.3390/su10072541.

SCCER-SoE, 2020. Swiss Potential for Hydropower Generation and Storage. Technical Report. SCCER-SoE.

Schildhauer, T.J., 2018. Biosynthetic Natural Gas (Bio-SNG). Springer New York, New York, NY. pp. 1–17. URL: https://doi.org/10.1007/978-1-4939-2493-6_996-1, doi:10.1007/978-1-4939-2493-6_996-1.

Schluck, T., Streicher, K.N., Mennel, S., 2019. Statistical modelling of the energy reference area based on the Swiss building stock. Journal of Physics: Conference Series 1343, 012031. doi:10.1088/1742-6596/1343/1/012031.

SECO, 2018. Langfristszenarien BIP 2018–2065. Data provided by the BFE.

Streicher, K., Allan, J., Murray, P., Bollinger, A., Marcucci, A., 2020a. Energy Efficiency from buildings retrofitting. Technical Report. U. Geneva, EMPA and ETH Zurich - JASM. URL: https://sccer-jasm.ch/JASMpapers/JASM_energyEfficiency_buildings.pdf.

Streicher, K.N., Mennel, S., Chambers, J., Parra, D., Patel, M.K., 2020b. Cost-effectiveness of large-scale deep energy retrofit packages for residential buildings under different economic assessment approaches. Energy and Buildings 215, 109870. URL: http://www.sciencedirect.com/science/article/pii/S0378778819333225, doi:https://doi.org/10.1016/j.enbuild.2020.109870.

SwissSolar, 2019. Faktenblatt: Strom von der Sonne. URL: https://www.swissolar.ch/fileadmin/user_upload/Solarenergie/Fakten-und-Zahlen/Branchen-Faktenblatt_PV_CH_d.pdf.

Thees, O., Burg, V., Erni, M., Bowman, G., Lemm, R., 2017. Biomass for Swiss Energy Transition SCCER-BIOSWEET. Technical Report. Swiss Federal Institute for Forest, Snow and Landscape Research WSL / Swiss Competence Center for Energy Research. URL: https://www.envidat.ch/ui/#/metadata/swiss-biomass-potentials, doi:10.16904/18.

VSE, 2012. Wege in die neue stromzukunft.

Walch, A., Castello, R., Mohajeri, N., Scartezzini, J.L., 2020. Big data mining for the estimation of hourly rooftop photovoltaic potential and its uncertainty. Applied Energy 262, 114404. URL: http://www.sciencedirect.com/science/article/pii/S0306261919320914, doi:https://doi.org/10.1016/j.apenergy.2019.114404.

Walch, A., Mohajeri, N., Scartezzini, J.L., 2019. A critical comparison of methods to estimate solar rooftop photovoltaic potential in switzerland. Journal of Physics: Conference Series 1343, 012035. doi:10.1088/1742-6596/1343/1/012035.

WEC, 2019. World Energy Scenarios 2019 – Exploring Innovation Pathways to 2040. Technical Report. World Energy Council. URL: https://www.worldenergy.org/publications/entry/world-energy-scenarios-2019-exploring-innovation-pathways-to-2040.

Witte, J., Kunz, A., Biollaz, S.M., Schildhauer, T.J., 2018. Direct catalytic methanation of biogas – part ii: Techno-economic process assessment and feasibility reflections. Energy Conversion and Management 178, 26 – 43. URL: http://www.sciencedirect.com/science/article/pii/S0196890418310884, doi:https://doi.org/10.1016/j.enconman.2018.09.079.

Wüest Partner, 2019. Entwicklung Energiebezugsflächen EBF 1990-2019, jährliches update. URL: https://www.bfe.admin.ch/bfe/en/home/supply/statistics-and-geodata/energy-statistics/analysis-of-energy-consumption-by-specific-use.html.

Yilmaz, S., Murray, P., Bollinger, A., Guidati, G., 2020. Hourly demand profiles. Technical Report. U. Geneva and EMPA - JASM. URL: https://sccer-jasm.ch/JASMpapers/JASM_time_series.pdf.

Zuberi, M.J.S., Bless, F., Chambers, J., Arpagaus, C., Bertsch, S.S., Patel, M.K., 2018. Excess heat recovery: An invisible energy resource for the swiss industry sector. Applied Energy 228, 390 – 408. URL: http://www.sciencedirect.com/science/article/pii/S0306261918309395, doi:https://doi.org/10.1016/j.apenergy.2018.06.070.

Zuberi, M.J.S., Li, X., Wallerand, A.S., Maréchal, F., Patel, M.K., 2020. Energy Efficiency in industry. Technical Report. U. Geneva and EPFL - JASM. URL: https://sccer-jasm.ch/JASMpapers/JASM_energyEfficiency_industry.pdf.

Zuberi, M.J.S., Patel, M.K., 2017. Bottom-up analysis of energy efficiency improvement and co2 emission reduction potentials in the swiss cement industry. Journal of Cleaner Production 142, 4294 – 4309. URL: http://www.sciencedirect.com/science/article/pii/S0959652616320406, doi:https://doi.org/10.1016/j.jclepro.2016.11.178.

Zuberi, M.J.S., Patel, M.K., 2019. Cost-effectiveness analysis of energy efficiency measures in the swiss chemical and pharmaceutical industry. International Journal of Energy Research 43, 313–336. URL: https://onlinelibrary.wiley.com/doi/abs/10.1002/er.4267, doi:https://doi.org/10.1002/er.4267.

Zuberi, M.J.S., Tijdink, A., Patel, M.K., 2017. Techno-economic analysis of energy efficiency improvement in electric motor driven systems in swiss industry. Applied Energy 205, 85 – 104. URL: http://www.sciencedirect.com/science/article/pii/S030626191730987X, doi:https://doi.org/10.1016/j.apenergy.2017.07.121.